



Cite this: *RSC Adv.*, 2026, **16**, 1509

## Unlocking the potential of mandelic acid derivatives: chemical and biological applications – a comprehensive review†

Amit Banerjee<sup>a</sup> and Amrit Krishna Mitra   <sup>\*b</sup>

Mandelic acid, an aromatic  $\alpha$ -hydroxy acid first identified in 1831, has become a valuable scaffold in synthetic, medicinal, and industrial chemistry. Its aromatic ring, carboxylic acid group, and stereogenic centre provide a rare combination of chemical reactivity and stereochemical control, enabling the creation of structurally diverse and biologically active molecules. Enantiomer-specific derivatives find targeted pharmaceutical uses, with the *R*-form applied in the synthesis of cephalosporins, penicillin, anticancer agents, and anti-obesity drugs, and the *S*-form in the preparation of nonsteroidal anti-inflammatory agents. Beyond therapeutics, mandelic acid derivatives are important in catalysis, chiral separations, cosmetics, analytical chemistry, and materials science. They display a wide spectrum of biological activities, including antimicrobial, antiviral, antifungal, anticancer, anti-inflammatory, and enzyme-inhibitory properties, often enhanced through incorporation into heterocycles, hybrid frameworks, and polymeric systems. This review consolidates advances in the synthesis of bioactive derivatives such as factor Xa inhibitors, anti-HIV agents, dual-action anti-inflammatory and antimicrobial compounds, pyrazole–mandelic acid hybrids, thiazolidinone-based carbonic anhydrase IX inhibitors, oxadiazothioether antifungal agents, and plant pathogen virulence disruptors. It also highlights catalytic roles, separation technologies, and advanced material applications. Structure–activity relationship insights, emerging trends, and key challenges are discussed to guide the rational design of next-generation mandelic acid derivatives with enhanced chemical and biological potential.

Received 28th September 2025  
 Accepted 12th December 2025

DOI: 10.1039/d5ra07369c  
[rsc.li/rsc-advances](http://rsc.li/rsc-advances)

<sup>a</sup>Department of Chemistry, National Institute of Technology Sikkim, Ravangla, Sikkim 737139, India

<sup>b</sup>Department of Chemistry, Government General Degree College, Singur, Hooghly, West Bengal, 712409, India. E-mail: [amritsepistles@gmail.com](mailto:amritsepistles@gmail.com); Tel: +91-33-2630-0126; +91 9432164011



Amit Banerjee

Amit Banerjee obtained his BSc from the University of Calcutta, India, where he developed a strong interest in organic chemistry, under the guidance of Dr Amrit Krishna Mitra. He then pursued his MSc at the National Institute of Technology Sikkim, India. He had completed his MSc project work under the supervision of Dr Sumit Saha, working on the Total Synthesis of Macrolides.



Amrit Krishna Mitra

† This article is dedicated by Amrit Krishna Mitra to Prof. Ashutosh Ghosh on the occasion of his assuming the office of the Vice-Chancellor of the University of Calcutta.

Amrit Krishna Mitra, Group-A officer of the West Bengal Education Service, is an Assistant Professor of Chemistry at Government General Degree College, Singur, under the University of Burdwan, where he also served as the founder Head of the Department. He additionally held the charge of Controller of Examinations at Rani Rashmoni Green University from October, 2023 to August, 2025. He earned his BSc from St. Xavier's College, Kolkata, MSc from IIT Kharagpur, and PhD in Organic Chemistry from the University of Calcutta. With over 45 publications in reputed international journals and publishing houses, along with a book to his credit, his research interests include synthetic organic chemistry, photophysics, and chemistry education. He represented India as the Scientific Observer of the national delegation at the International Chemistry Olympiads in 2024 and 2025.



# 1 Introduction

Ferdinand Ludwig Winckler, a German pharmacist, first isolated mandelic acid from bitter almonds in 1831.<sup>1</sup> Since then, this aromatic  $\alpha$ -hydroxy acid and its derivatives have evolved into indispensable motifs in synthetic, medicinal, and industrial chemistry. As a key member of the  $\alpha$ -hydroxy acid family, mandelic acid functions both as a versatile chiral building block and as an effective resolving agent. Its enantiomers exhibit distinct synthetic utilities: (*R*)(*–*)-mandelic acid derivatives serve as chiral synthons in the preparation of semi-synthetic cephalosporins, penicillins, anticancer agents, and anti-obesity drugs, while (*S*)-mandelic acid finds widespread use in the synthesis of nonsteroidal anti-inflammatory drugs such as celecoxib and celecoxib.<sup>2,3</sup>

At the core of its importance lies the unique molecular architecture of mandelic acid, which combines an aromatic ring with a carboxylic acid group and a stereogenic  $\alpha$ -hydroxyl centre. This arrangement endows the molecule with a rare convergence of chirality, hydrogen-bonding capacity, redox responsiveness, and acid–base tunability. The  $\alpha$ -hydroxyl group provides nucleophilicity and metal-coordination ability, while the benzylic position enables controlled oxidation, substitution, and esterification reactions. The aromatic ring further allows

electronic modulation through substituents, enabling precise tuning of lipophilicity, acidity, and biological interactions. Importantly, the inherent stereogenic centre makes mandelic acid a privileged chiral synthon: both enantiomers are readily accessible, configurationally stable, and compatible with diverse asymmetric transformations, making them invaluable in enolate chemistry, asymmetric catalysis, and chiral auxiliary design.<sup>4</sup> These combined features distinguish mandelic acid as a privileged scaffold, capable of engaging in multiple reaction pathways while offering predictable stereochemical outcomes—traits that few small molecules simultaneously possess.

To provide a clear structural overview for readers particularly those less familiar with the chemistry of  $\alpha$ -hydroxy acids, a schematic representation has been included as Fig. 1, depicting the fundamental molecular framework of mandelic acid together with a selection of its most prominent derivative classes. This figure illustrates how simple structural modifications, such as esterification or amidation, as well as more advanced transformations including aryl substitutions, polymerization, ionic-liquid formation, and heterocycle hybridization (e.g., pyrazole-, oxadiazole-, phthalimide-, and thiazolidinone-based derivatives), systematically diversify the physicochemical and biological attributes of the parent scaffold. By visually mapping these representative derivative

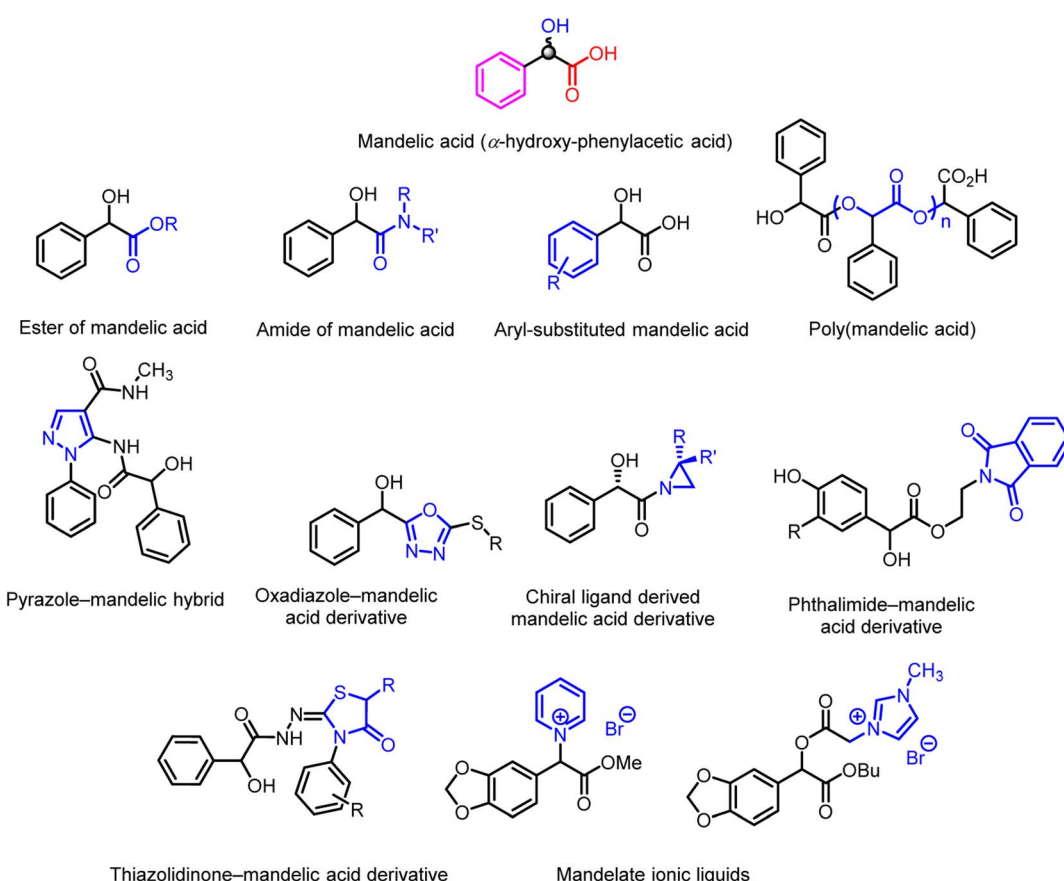


**Fig. 1** Structural framework of mandelic acid and major categories of its derivatives, including ester, amide, aryl-substituted, polymeric, ionic-liquid, and heterocycle-hybrid forms. These examples highlight the chemical flexibility of the scaffold and its relevance across diverse functional applications.



categories, the figure serves as an accessible guide to the extensive chemical space covered in this review and establishes a structural context for understanding the wide-ranging synthetic strategies and multifunctional properties discussed in the following sections.

Although mandelic acid occurs naturally in certain botanical sources, its high synthetic accessibility has facilitated its integration across pharmaceuticals, cosmetics, analytical chemistry, catalysis, polymer science, and materials engineering.<sup>5–11</sup> Over the past decades, derivatives of mandelic acid have demonstrated impressive biological versatility, exhibiting antimicrobial, antiviral, anticancer, antifungal, anti-inflammatory, enzyme-inhibitory, and even phytoprotective activities.<sup>12–16</sup> Their structural flexibility allows seamless incorporation into heterocycles, molecular hybrids, and polymeric networks, enabling the design of next-generation therapeutics targeting infectious diseases, metabolic disorders, inflammation, and cancer. Concurrently, their relevance in chemical sciences remains profound; they continue to function as robust chiral auxiliaries, catalytic components, and precursors for architecturally complex molecules.<sup>5,9,11,13,14</sup>

Despite being a classical scaffold, the last decade has witnessed a profound expansion in the chemical and biological landscape of mandelic acid derivatives, necessitating a contemporary and critical reassessment. Existing reviews are either dated or narrow in scope—focusing primarily on classical synthetic routes, specific subclasses of derivatives, or isolated biomedical uses. These earlier works do not account for the remarkable post-2015 advances that have transformed this domain, including transition-metal-catalysed C–H activation, biocatalytic oxidative strategies, enantioselective enolate-based methodologies, ionic-liquid derivatives, and an expanding repertoire of multifunctional hybrid scaffolds (e.g., pyrazole-mandelic, oxadiazole-mandelic, and thiazolidinone-mandelic systems). Equally significant are the broadened application frontiers: modern factor Xa inhibitors, anti-HIV agents, dual-action anti-inflammatory/antimicrobial compounds, plant-pathogen virulence disruptors, chiral ligands, organometallic complexes, and polymer-supported materials. Collectively, these developments signify a paradigm shift in how mandelic acid derivatives are conceptualized, synthesized, and applied—yet the literature lacks a unified source capturing these diverse advancements.

In this context, an up-to-date and integrative review is essential to consolidate modern progress, elucidate emerging structure–activity relationships (SAR), and illustrate how contemporary synthetic innovations have reshaped the biological and chemical potential of mandelic acid derivatives. This review addresses that need by offering a comprehensive and critical overview of recent developments spanning synthetic methodologies, therapeutic applications, catalytic transformations, and advanced materials. It highlights how functional group manipulation and strategic hybridization have driven both chemical diversity and biological potency. Finally, it outlines key challenges, unresolved questions, and future opportunities that may guide the next wave of mandelic-acid-based discovery.

## 2 Methodology

This review was compiled through a comprehensive and systematic survey of the literature on mandelic acid and its derivatives, with a focus on both chemical and biological applications. A multi-database search strategy was employed, covering Web of Science, Scopus, PubMed, ScienceDirect, and Google Scholar to ensure broad coverage of peer-reviewed articles, patents, and relevant conference proceedings. Keywords used in various combinations included mandelic acid, mandelic acid derivatives, synthesis, factor Xa inhibitors, anti-HIV agents, dual-action anti-inflammatory antimicrobial compounds, pyrazole–mandelic hybrids, carbonic anhydrase IX inhibitors, oxadiazothioether antifungal agents, *Ralstonia solanacearum* virulence inhibition, catalysis, enantioselective separation, and materials science applications.

The literature search was restricted primarily to publications from 2000 to 2025, while earlier landmark studies were also incorporated to provide historical context. Studies were included if they reported synthetic methodologies, biological evaluation, structure–activity relationship (SAR) analysis, or chemical applications of mandelic acid derivatives. Articles lacking sufficient experimental detail, reproducibility, or clear relevance were excluded.

Data from eligible studies were extracted and organized according to thematic categories reflecting the major research domains: (i) synthesis of derivatives with biological activities, (ii) design of derivatives for targeted therapeutic applications, (iii) structural modification for enhanced biological potency, (iv) synthesis of derivatives for chemical and material science applications, and (v) SAR-based insights guiding future developments. Where applicable, comparative analyses were performed to highlight trends in synthetic strategies, biological activities, and application potential.

This structured approach ensured that the review provides a balanced, up-to-date, and cross-disciplinary synthesis of current advances, offering valuable insights for chemists, pharmacologists, and material scientists engaged in mandelic acid-based research.<sup>17–19</sup>

## 3 Mandelic acid derivatives possessing biological applications

Mandelic acid and its derivatives form a versatile class of  $\alpha$ -hydroxy aromatic acids with significant relevance in medicinal and agrochemical research. Their biological potential stems from the scaffold's modifiable aromatic ring, stereogenic center, and functional groups, which enable diverse interactions with biological targets. Over the past decade, strategic structural modifications—such as heterocycle incorporation, hybrid formation, and side-chain tuning—have expanded the pharmacological spectrum of mandelic acid derivatives. This section highlights representative examples, key structure–activity relationships (SAR), and emerging applications, with a focus on concise mechanistic insights rather than exhaustive experimental detail.

### 3.1. Mandelic acid derivatives as potent and selective factor Xa inhibitors

Factor Xa is a trypsin-like serine protease positioned at a crucial junction of the intrinsic and extrinsic coagulation pathways, driving thrombin formation and, subsequently, fibrin generation. Owing to its central regulatory role, factor Xa has emerged as a validated therapeutic target for thromboembolic disorders.<sup>20-24</sup>

Su *et al.* (2001) reported monobasic non-covalent factor Xa inhibitors derived from mandelic acid that incorporate a benzamidine moiety.<sup>25</sup> Their design strategy focused on lowering overall basicity while maintaining strong interactions with the S1 and S4 subpockets of the enzyme. Structural modifications around the mandelic acid aromatic ring, particularly the introduction of electron-withdrawing or hydrophobic substituents, led to enhanced potency by improving complementary fit within the hydrophobic S4 region and maintaining benzamidine-Asp-189 interactions in S1.<sup>20,25</sup>

Representative analogues (Compounds 1 family and Compound 2) demonstrated significant antithrombotic activity and high selectivity over thrombin and trypsin (Fig. 2).

The key SAR insight is that modifying the aromatic ring of mandelic acid, such as by introducing electron-withdrawing or hydrophobic substituents, enhances its ability to align with the S1 and S4 pockets of factor Xa, thereby improving binding affinity and inhibitory potency.

### 3.2. Engineering anti-HIV-1 agents through the therapeutic promise of poly(mandelic acid) derivatives

Poly(mandelic acid) (PMDA) (4), derived from the chiral monomer mandelic acid (MDA), has attracted attention due to its biocompatibility and previous clinical relevance of MDA-based drugs such as methenamine mandelate.<sup>26-28</sup> Motivated by these pharmacological foundations, polymeric mandelate analogues are being explored for antiviral applications.

In 2007, Ward and colleagues evaluated the anti-HIV-1 potential of poly(mandelic acid) (PMDA) (4) synthesized *via* three distinct methods<sup>29</sup> (Fig. 3). Notably, only the polymer produced using concentrated sulfuric acid as a catalyst showed promising antiviral activity. This specific variant was subsequently designated as Sulfuric Acid Modified Mandelic Acid (SAMMA), although its structural features appeared to differ from conventional polyester-like frameworks previously proposed. Further investigations revealed that PMDAs obtained through acid-catalyzed step-growth polymerization exhibited significant inhibitory effects against both HIV-1 and herpes

simplex virus (HSV). The XRF profile of poly(sodium styrenesulfonate) (3) was recorded, as this polymer served as a standard reference material for evaluating the PMDA sample in the researchers' analysis.

To better understand the relationship between polymer structure and biological efficacy, this study explored how both the synthetic route and the stereochemical configuration influence PMDA's anti-HIV-1 activity. Since PMDAs (or SAMMA, as referenced in earlier reports) have demonstrated potential as topical microbicides, it becomes critical to accurately identify the biologically active form. However, inconsistencies in existing literature regarding the actual structure of the active material have led to ambiguity. Clarifying the composition of these functional polymers is therefore essential for advancing their development as antiviral agents.

While PMDA derivatives highlight the therapeutic promise of polymeric scaffolds in antiviral research, their ambiguous structural identity and variable efficacy reflect a recurring challenge in mandelic acid chemistry: translating diverse structural modifications into predictable and reproducible biological outcomes. This limitation has prompted researchers to explore alternative strategies that combine mandelic acid with other well-established pharmacophores to achieve multifunctionality. In this context, hybrid frameworks such as mandelic acid-based phthalimides represent a logical progression, leveraging the individual strengths of both scaffolds to design dual-action agents capable of addressing complex clinical challenges like drug resistance and inflammatory disorders.

The key structural insight is that differences in the polymer structure produced by different synthesis methods directly influence antiviral potency, with sulfuric acid-derived PMDA showing the highest activity.

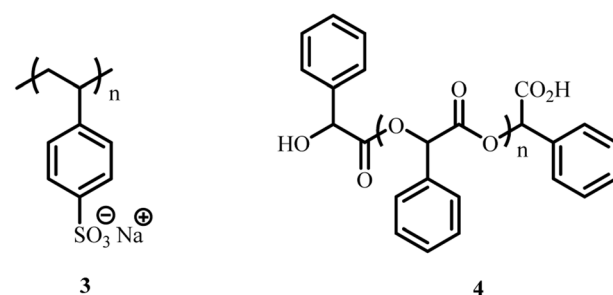


Fig. 3 Representative structures of poly(sodium styrenesulfonate) (3) and poly(mandelic acid) (4), adapted from ref. 29 with permission from [ACS] [Ward *et al.*, 2007], copyright 2007.

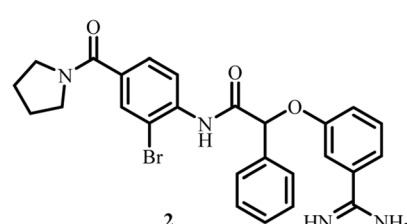
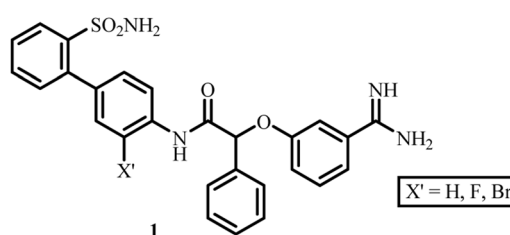


Fig. 2 Compounds 1 analogues, and 2, possessing enzyme inhibitory centres structurally akin to serine proteases, thrombin and trypsin 25.



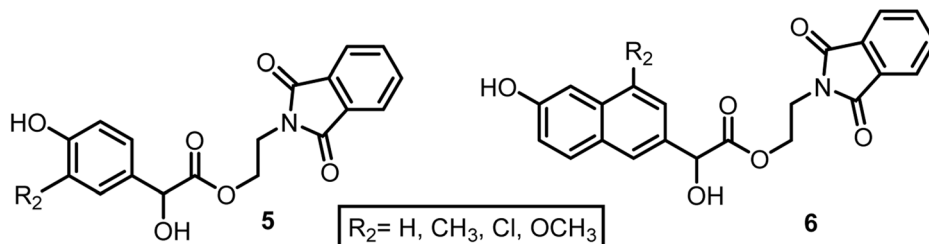


Fig. 4 Structures of the active antibacterial compounds 5 and 6<sup>33</sup>

### 3.3. Mandelic acid-based phthalimides as promising dual-action agents against inflammation and microbial infections

Mandelic acid and phthalimide scaffolds each exhibit a wide range of pharmacological activities, including antimicrobial, antioxidant, and anti-inflammatory effects.<sup>6,30-32</sup> To combine these properties in a single framework, Varala *et al.* (2008) designed mandelic acid–phthalimide hybrids aimed at simultaneously addressing microbial infections and inflammation, an advantage in disorders where secondary infection exacerbates inflammatory responses.<sup>33</sup> Representative structures of these hybrids are shown in Fig. 4.

The antibacterial activity of compounds 5 and 6 was evaluated against *Staphylococcus aureus*, *Bacillus cereus*, *Escherichia coli*, and *Klebsiella pneumoniae*, while antifungal testing was conducted against *Candida albicans* and *Aspergillus niger*. Antimicrobial potency was measured using the paper disc diffusion assay, and MIC values were determined via agar streak dilution. All synthesized derivatives also displayed noteworthy anti-inflammatory activity, with several approaching the efficacy of indomethacin. Some compounds effectively reduced paw edema and were reported to be non-toxic and safe, supporting their potential for therapeutic application, including oral administration.

Building on the promising dual-action properties of mandelic acid-based phthalimides, further structural innovation has led to the development of amide hybrids that integrate the pyrazole framework with mandelic acid. These hybrids offer new avenues to enhance therapeutic efficacy through synergistic bioactivity and targeted molecular design.

The key SAR insight is that the incorporation of the phthalimide ring enhances both antimicrobial and anti-inflammatory potency by improving  $\pi$ - $\pi$  stacking and biological target engagement, while hydrophobic substituents on the mandelate ring further strengthen activity, likely through enhanced membrane permeation.

### 3.4. Unlocking the therapeutic potential through the synthesis and bio-evaluation of amide hybrids featuring pyrazole-mandelic acid frameworks

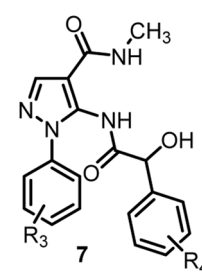
Stan *et al.* (2004, 2015) evaluated the antimicrobial and preservative efficacy of oxyacetyl mandelic acid and oxypropionyl mandelic acid in ointment formulations.<sup>34</sup> Both derivatives showed strong antibacterial and antifungal activity at low concentrations against *Staphylococcus aureus*, *Pseudomonas aeruginosa*, *Candida albicans*, *Escherichia coli*, *Aerobacter aerogenes*,

and other pathogens. They significantly reduced fungal colony counts and inhibited the growth of both Gram-positive and Gram-negative bacteria within two days of inoculation.

Building on these observations, amide derivatives, well known for their pharmaceutical and agrochemical utility and pyrazoles, a privileged scaffold with established antibacterial, antifungal, and antiviral properties,<sup>36–41</sup> offer valuable opportunities for hybrid design. Incorporating these features into the mandelic acid framework, itself a component of agrochemical agents such as Mandipropamid (**14**), enables the development of multifunctional molecules with broadened activity profiles.<sup>35</sup>

In 2017, Xie *et al.* reported a series of pyrazole amide derivatives incorporating mandelic acid moieties and assessed their antiviral effects against Tobacco Mosaic Virus (TMV).<sup>42</sup> Sixteen derivatives of *N*-methyl-1*H*-pyrazole-4-acetyl methylamine (7), bearing various 1-substituted phenyl and 5-(2-substituted phenyl-2-hydroxyethyl amide) groups, were synthesized and evaluated *in vivo*. Several compounds displayed enhanced antiviral activity in the standard half-leaf bioassay, with Ningnanmycin used as the positive control. Structure–activity analysis indicated that electron-withdrawing substituents on the mandelate aromatic ring, particularly *para*-fluoro (*p*-F) and *para*-chloro (*p*-Cl) substantially improved anti-TMV efficacy. These groups likely promote stronger target interactions and better cell permeability, accounting for the superior activity of the *p*-F and *p*-Cl derivatives (Fig. 5).

The study of pyrazole-mandelic acid hybrids demonstrates how rational structural design can broaden the utility of mandelic acid derivatives from antimicrobial and antiviral agents to agrochemicals. Despite their strong bioactivity, many such hybrids remain target-specific, prompting interest in whether



$R_3 = p\text{-F, } p\text{-Cl, } p\text{-Br, } m\text{-Br, H}$   
 $R_4 = o\text{-F, } o\text{-Cl, } p\text{-Cl, H}$

Fig. 5 Structure of compound 7 exhibiting antiviral activity against TMV.<sup>42</sup>

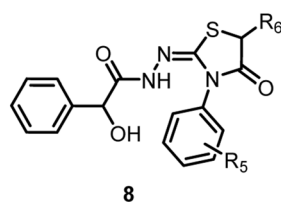
mandelic acid scaffolds can also address complex diseases such as cancer. This transition from pathogen or crop protection to oncology underscores the versatility of mandelic acid chemistry and the value of scaffold diversification. In this direction, the development of thiazolidinone-based mandelic acid derivatives as selective hCA IX inhibitors exemplifies how mandelic acid can be incorporated into non-traditional pharmacophores to yield safer, more selective compounds relevant to tumour biology.

### 3.5. Development of novel thiazolidinone-based mandelic acid derivatives as potent human carbonic anhydrase IX inhibitors

Recent work has expanded the therapeutic relevance of mandelic acid derivatives to oncology, particularly through the inhibition of human Carbonic Anhydrase IX (hCA IX), an isoform overexpressed in hypoxic tumours and closely linked to cancer progression.<sup>43–46</sup> Carbonic Anhydrases (CAs) are metalloenzymes that regulate respiration and pH homeostasis by catalysing the reversible hydration of  $\text{CO}_2$  to bicarbonate and protons.<sup>43</sup> Among the CA isoforms, hCA IX is distinguished by its strong expression in solid hypoxic tumours, where it supports tumour growth by maintaining an acidic extracellular milieu favourable to cancer cell survival and invasion.<sup>43–46</sup> This has positioned hCA IX as a compelling target for anticancer drug development.

Although many potent hCA IX inhibitors, most notably sulphonamide-based compounds, have been reported,<sup>47–50</sup> these agents often suffer from adverse effects such as haematological toxicity, allergic reactions, and susceptibility to infection. Sulphonamide CAIs typically inhibit the enzyme by coordinating directly to the active-site  $\text{Zn}^{2+}$  via a zinc-binding group (ZBG). To address issues of selectivity and tolerability, alternative strategies have explored inhibitors that interact with allosteric regions or engage the active site without direct zinc coordination.<sup>51</sup>

In light of these challenges, Güzel-Akdemir and co-workers (2018) investigated a novel class of hCA IX inhibitors based on the 4-thiazolidinone scaffold, known for its favourable safety profile, good bioavailability, and diverse biological activities.<sup>52</sup> These newly synthesized thiazolidinone-based mandelic acid derivatives (8) (Fig. 6), notably devoid of the classical sulphonamide ZBG, demonstrated low micromolar inhibitory activity against hCA IX. Molecular docking studies further revealed that these compounds inhibit the enzyme without directly interacting with the zinc ion in the active site, suggesting a non-classical inhibition mechanism.



$\text{R}_5 = \text{CH}_3, \text{OCH}_3, \text{NO}_2, \text{F}, \text{Cl}, \text{Br}, \text{CF}_3$   
 $\text{R}_6 = \text{H}, \text{CH}_3$

Fig. 6 Structure of compound 8 showing inhibitory activity against hCA IX.<sup>52</sup>

Building on the design of thiazolidinone-based mandelic acid derivatives with potent enzyme inhibitory activity, attention has also turned to novel mandelic acid analogues incorporating 1,3,4-oxadiazothioether moieties. These compounds have shown considerable promise as antifungal agents, further demonstrating the diverse bioactive potential of mandelic acid frameworks. The key SAR insights indicate that the thiazolidinone ring serves as an effective pharmacophore for hCA IX recognition, while aryl substituents on the mandelate moiety modulate lipophilicity and  $\pi$ -interactions, thereby strengthening target binding and enhancing inhibitory potency.

### 3.6. Exploring novel mandelic acid derivatives featuring 1,3,4-oxadiazothioether for promising antifungal activity

Wu *et al.* in 2021 developed and crafted a range of innovative mandelic acid derivatives, incorporating a 1,3,4-oxadiazole-thioether moiety (13) (Scheme 1).<sup>53</sup> Bioassay investigations revealed that specific target molecules exhibited notable *in vitro* antifungal activity against six types of pathogenic fungi. Compounds containing substituents,  $\text{R}_7 = (\text{CH}_2)_4\text{CH}_3$  and  $\text{R}_7 = 4\text{-methylbenzyl}$ , demonstrated activity against *Gibberella saubinetii* and *Sclerotinia sclerotiorum*.

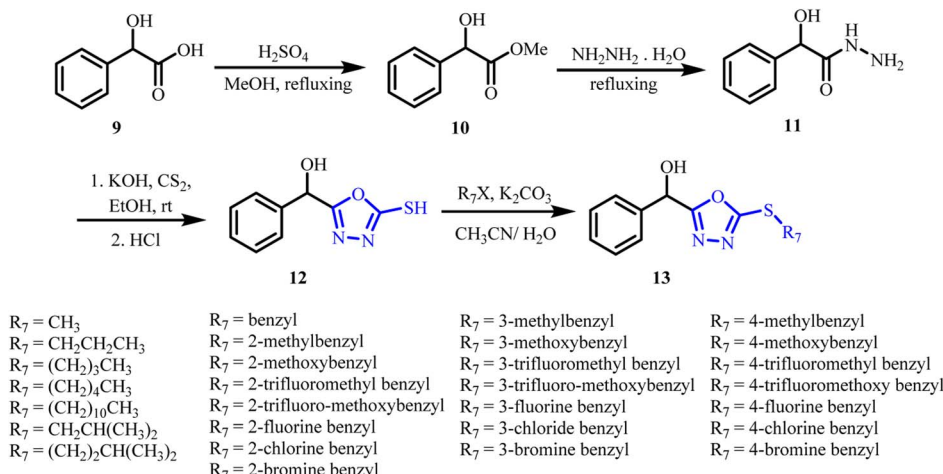
In order to investigate the influence of the spatial arrangement of the compounds on their biological activity, a set of chiral mandelic acid derivatives with a 1,3,4-oxadiazole thioether moiety (13) were created and manufactured by Hou *et al.* in 2023, stepping on the same pathway discussed in Scheme 1.<sup>54</sup> The majority of compounds with the *S*-configuration showed increased *in vitro* antifungal activity against three plant fungus, according to the results of the bioassay.

In 2023, Shi *et al.* applied the same synthetic strategy outlined in Scheme 1 to identify novel lead compounds targeting *Thanatephorus cucumeris*.<sup>55</sup> Their investigation demonstrated that the compound bearing a 2-methylbenzyl substituent at the  $\text{R}_7$  position exhibited remarkable antifungal activity against *T. cucumeris* mycelia. This compound compromised the structural integrity of the fungal cell membrane, leading to increased membrane permeability. As a result, intracellular electrolytes were released, effectively inhibiting fungal growth. This study offers valuable insights toward the development of effective agents for managing rice sheath blight caused by *T. cucumeris*.

In the pursuit of effective plant fungicides, Chen *et al.* (2023) adopted a similar strategy (Scheme 1) to design and synthesize a series of 4-substituted mandelic acid derivatives incorporating a 1,3,4-oxadiazole moiety (15) (Fig. 7b).<sup>56</sup> *In vitro* bioassays revealed that several of these compounds exhibited notable antifungal activity against *Gibberella saubinetii*, *Verticillium dahliae*, and *Sclerotinia sclerotiorum*. Remarkably, their efficacy surpassed that of the commercial fungicide Mandipropamid (Fig. 7a). Further investigations using fluorescence and scanning electron microscopy confirmed that these compounds compromised hyphal surface structure, disrupted membrane integrity, and effectively inhibited fungal cell proliferation.

Following the promising antifungal properties of mandelic acid derivatives containing 1,3,4-oxadiazothioether moieties, recent research has expanded to explore their potential in combating





**Scheme 1** Synthetic route to mandelic acid derivatives incorporating a 1,3,4-oxadiazole-thioether moiety, adapted from ref. 54 with permission from [ACS] [Hou *et al.*, 2023], copyright 2023.

bacterial plant pathogens. Notably, novel mandelic acid derivatives have been developed that disrupt the virulence of *Ralstonia solanacearum* by targeting its type III secretion system, highlighting the compound's emerging role in agricultural disease management.

### 3.7. Novel mandelic acid heterocyclic hybrids: expanding anti-virulence, antimycobacterial, anticancer, and agrochemical applications

Beyond their antifungal properties, mandelic acid derivatives incorporating heterocyclic pharmacophores have recently garnered significant interest due to their anti-virulence, antimycobacterial, anticancer, and agrochemical applications.

Cui *et al.* (2023) reported mandelic acid derivatives bearing a 2-mercaptop-1,3,4-thiazole scaffold (**18**) as inhibitors of the type III secretion system (T3SS) in *Ralstonia solanacearum*, a major phytopathogen (Scheme 2).<sup>57</sup> The 4-fluorobenzyl analogue ( $R_{10} = 4\text{-fluorobenzyl}$ ) significantly suppressed the transcription of the *hrpY* gene and effectively blocked the type III secretion system. Impressively, this compound outperformed previously reported inhibitors without adversely affecting the bacterial growth, highlighting its potential as a selective anti-virulence agent.

*Citrus canker*, caused by *Xanthomonas citri* subsp. *citri* (Xcc), is another destructive plant disease where T3SS plays a critical role.<sup>58-63</sup> T3SS inhibitors specifically block the structure or function of this system without affecting bacterial growth,

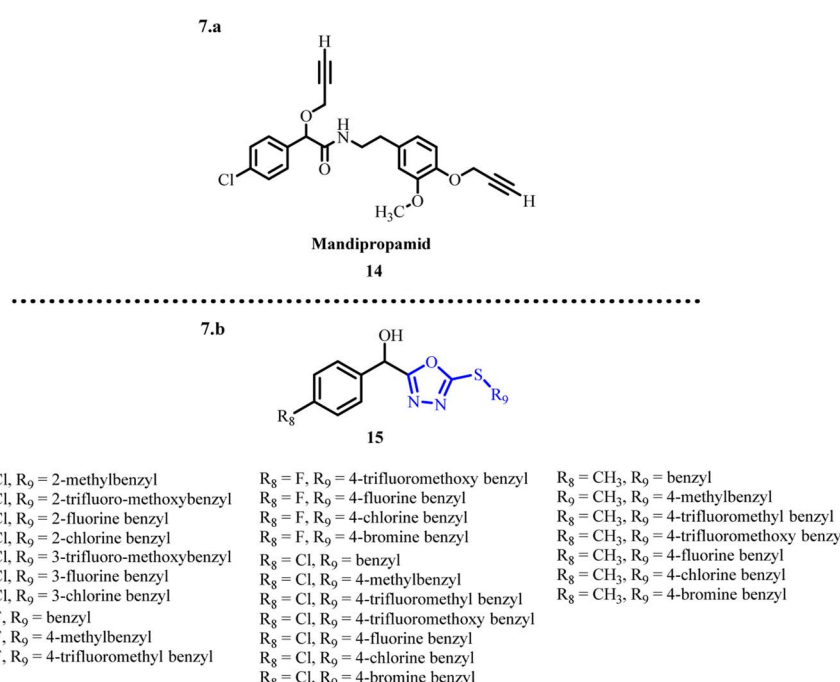


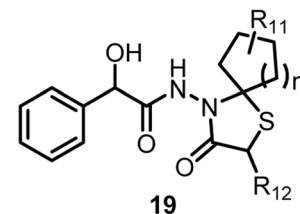
**Fig. 7** (a) Representative structure of the commercial fungicide Mandipropamid. (b) 4-substituted mandelic acid derivatives bearing a 1,3,4-oxadiazole moiety.<sup>56</sup>

offering a non-bactericidal yet effective strategy to combat infections caused by *Pseudomonas*, *Salmonella*, *Xanthomonas*, and others.<sup>64–68</sup>

To target this pathway, Cui *et al.* (2024) developed mandelic acid-2-mercaptop-1,3,4-thiadiazole hybrids (Scheme 2) that inhibited hypersensitive response and pathogenicity in *Xcc*.<sup>69</sup> The best-performing compound (2-methylbenzyl substitution) significantly suppressed T3SS-related genes and the citrus susceptibility gene *CsLOB1*, offering a promising non-bactericidal strategy for crop protection.

Tuberculosis remains a major global health concern, compounded by multidrug resistance and toxicity of existing regimens.<sup>70,71</sup> Given the essential roles of FAS-I and FAS-II pathways in mycolic acid biosynthesis,<sup>72–74</sup> spirothiazolidinone derivatives have emerged as attractive antimycobacterial agents.<sup>75–78</sup> Trawally *et al.* (2022) synthesized mandelic acid-based spirothiazolidinones (**19**) (Fig. 8), several of which exhibited up to 98% growth inhibition of *Mycobacterium tuberculosis* H37Rv at 6.25  $\mu\text{g mL}^{-1}$ . Preliminary mechanistic insights implicated targets such as HadAB, DprE1, Pks13, FadD32, and InhA are the key enzymes essential for cell-wall synthesis.<sup>79</sup>

Cancer continues to impose a heavy disease burden globally, necessitating safer and more effective treatment options.<sup>80–85</sup> Thiazolidin-4-ones are privileged anticancer scaffolds with broad-spectrum bioactivities.<sup>86–90</sup> In 2022, building upon their earlier studies, Kübra Demir-Yazıcı and co-workers set out to design a novel anticancer agent by merging two pharmacophores with known anticancer potential.<sup>92</sup> Specifically, they combined the mandelic acid moiety, **11** and **21** to possess promising anticancer activity,<sup>79</sup> with the 2-aryl-1,3-thiazolidin-4-one core found in compound **20**, a structure also recognized for its cytotoxic effects<sup>91</sup> (Fig. 9). This rational hybridization aimed to synergistically enhance biological efficacy and pave the way for the development of next-generation anticancer therapeutics.



**19**  
 $R_{11} = H, CH_3, 8-C_2H_5, 8-C_6H_5, 8-C_3H_7$   
 $R_{12} = H, CH_3$   
 $n = 1, 2$

Fig. 8 Structures of mandelic acid-based spirothiazolidinone derivatives.<sup>79</sup>

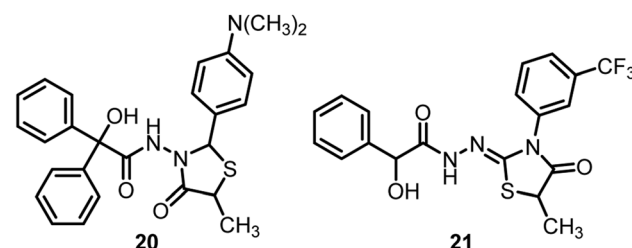
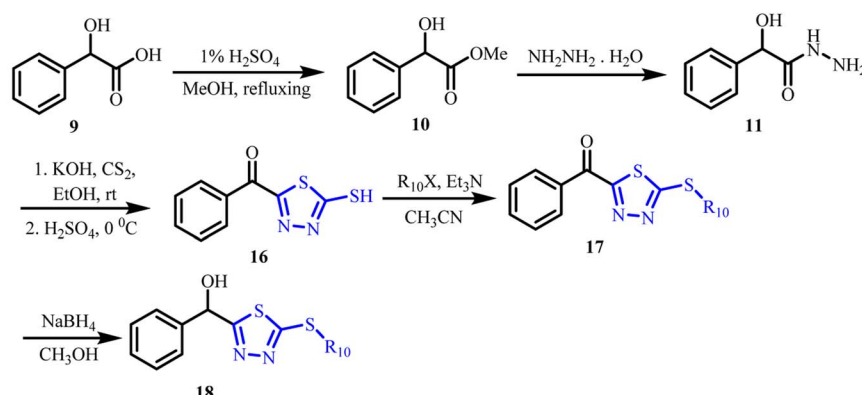


Fig. 9 Representative structures of active anticancer agents.<sup>92</sup>

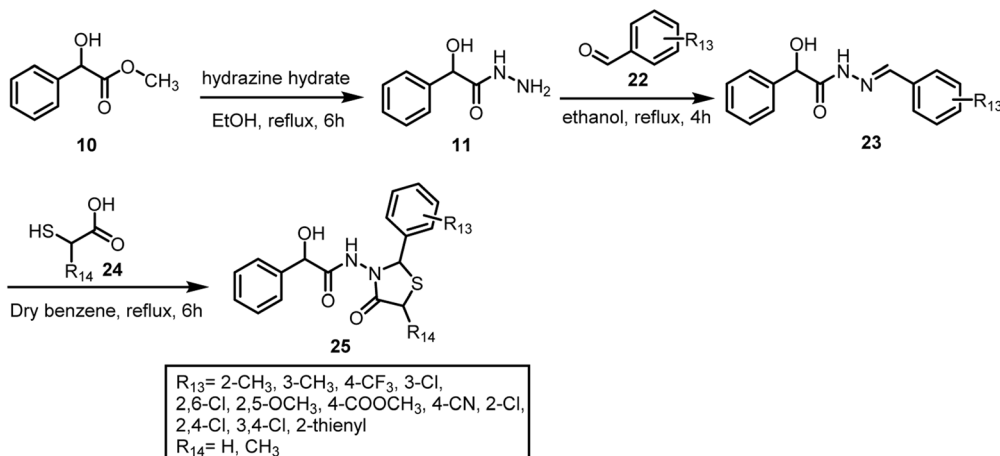
The researchers strategically designed their new molecular hybrids to incorporate the bioactive features of both compounds **20** and **21**, aiming to synergize their anticancer properties. Several of the synthesized derivatives (Scheme 3) demonstrated notable cytotoxicity against the melanoma cell line UACC-62. However, these compounds exhibited only moderate activity against other cancer cell lines, including leukemia (RPMI-266), non-small cell lung cancer (NCL-H23 and HOP-92), and ovarian cancer (IGROV1). Despite this variability,



$R_{10} = CH_3$	$R_{10} = benzyl$	$R_{10} = 3\text{-methylbenzyl}$	$R_{10} = 4\text{-methylbenzyl}$
$R_{10} = CH_2CH_3$	$R_{10} = 2\text{-methylbenzyl}$	$R_{10} = 3\text{-methoxybenzyl}$	$R_{10} = 4\text{-methoxybenzyl}$
$R_{10} = CH_2CH_2CH_3$	$R_{10} = 2\text{-methoxybenzyl}$	$R_{10} = 3\text{-trifluoromethyl benzyl}$	$R_{10} = 4\text{-trifluoromethyl benzyl}$
$R_{10} = (CH_2)_3CH_3$	$R_{10} = 2\text{-trifluoromethyl benzyl}$	$R_{10} = 3\text{-trifluoro-methoxybenzyl}$	$R_{10} = 4\text{-trifluoromethoxy benzyl}$
$R_{10} = (CH_2)_4CH_3$	$R_{10} = 2\text{-trifluoro-methoxybenzyl}$	$R_{10} = 3\text{-fluorine benzyl}$	$R_{10} = 4\text{-fluorine benzyl}$
$R_{10} = (CH_2)_5CH_3$	$R_{10} = 2\text{-fluorine benzyl}$	$R_{10} = 3\text{-chloride benzyl}$	$R_{10} = 4\text{-chlorine benzyl}$
$R_{10} = CH_2CH(CH_3)_2$	$R_{10} = 2\text{-chlorine benzyl}$	$R_{10} = 3\text{-bromine benzyl}$	$R_{10} = 4\text{-bromine benzyl}$
$R_{10} = (CH_2)_2CH(CH_3)_2$	$R_{10} = 2\text{-bromine benzyl}$		

Scheme 2 Synthetic route to mandelic acid derivatives incorporating a 2-mercaptop-1,3,4-thiadiazole moiety, adapted from ref. 69 with permission from [ACS] [Cui *et al.*, 2024], copyright 2024.



Scheme 3 Synthetic route for the preparation of compound 25.<sup>92</sup>

the *in vitro* assays yielded promising results, suggesting that these mandelic acid-based hybrids hold potential as effective anticancer agents, particularly against melanoma.

'Brown rot of stone fruit', caused by *Monilinia fructicola*, is a highly destructive fungal disease that severely impacts global stone fruit production.<sup>93–96</sup> The pathogen spreads rapidly *via* air- and water-borne conidia,<sup>97</sup> and despite routine use of commercial fungicides during bloom and pre-/post-harvest treatments, resistance development remains a growing concern.<sup>98</sup>

Piperazine scaffolds, particularly *N*-substituted derivatives, offer favourable physicochemical properties such as low toxicity, tunable lipophilicity, and strong hydrogen/ionic bonding capacity, making them valuable in medicinal chemistry.<sup>99–102</sup> However, their potential in agrochemical applications remains underexplored.

To address this, Wu *et al.* (2024) synthesized mandelic acid-piperazine hybrids as novel antifungal agents targeting *M. fructicola*.<sup>103</sup> These molecules exhibited potent activity *in vitro* ( $EC_{50} \approx 11.8 \text{ mg L}^{-1}$ ) and strong protective efficacy in post-harvest pear assays ( $\sim 200 \text{ mg L}^{-1}$ ). 3D-QSAR studies highlighted the critical influence of steric and electronic modulation at the  $R_{16}$  position (Fig. 10) on antifungal potency. Mechanistic investigations further revealed that these compounds

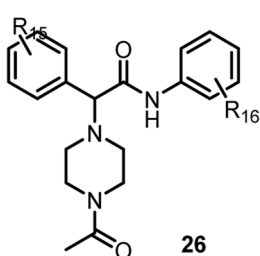
compromise fungal membrane integrity, elevate reactive oxygen species (ROS), and induce lipid peroxidation, as confirmed by increased malondialdehyde (MDA) levels. This work therefore establishes mandelic acid-piperazine hybrids (26) as promising, environmentally compatible fungicidal candidates for effective management of brown rot in stone fruit production.

Collectively, these findings demonstrate the versatility of mandelic acid as a privileged scaffold that can be strategically hybridized with thiazole, thiadiazole, thiazolidinone, and piperazine motifs to modulate diverse biological pathways, from T3SS inhibition and antimycobacterial action to selective anticancer and agrochemical outcomes. Such innovative molecular designs highlight the expanding translational value of mandelic acid frameworks and provide strong prospects for future therapeutic and crop-protection applications.

### 3.8. Discussion: biological promise of mandelic acid derivatives

Across the diverse examples presented in Sections 3.1–3.7, mandelic acid emerges as a privileged, modular scaffold whose biological performance is governed by a fine balance of electronic effects, stereochemistry, hydrophobic character and heterocyclic fusion. Rather than acting as a passive linker, the mandelate core actively participates in target recognition through its  $\alpha$ -hydroxy-aryl framework, which can be systematically tuned to optimise potency and selectivity.

A recurring SAR feature is the importance of aromatic ring substitution on the mandelate moiety. In factor Xa inhibitors, appropriate introduction of electron-withdrawing or hydrophobic substituents on the phenyl ring enhances complementarity with the S1 and S4 pockets, simultaneously preserving the benzamidine-Asp-189 interaction and improving overall binding affinity and selectivity over thrombin and trypsin (Section 3.1). Similarly, in pyrazole-mandelic acid antiviral hybrids, *para*-fluoro and *para*-chloro substituents on the mandelate ring markedly reinforce anti-TMV activity, consistent with an SAR model where electron-withdrawing groups improve target binding and cell permeability (Section 3.4). This electronic tuning principle extends into antifungal design, where 4-

Fig. 10 Representative structures of compound 26 analogues.<sup>103</sup>

substituted mandelic derivatives bearing 1,3,4-oxadiazole(thioether) motifs outperform Mandipropamid, again underscoring the role of para-substitution and overall aromatic electronics in modulating bioefficacy (Section 3.6).

Hydrophobic bulk and side-chain architecture also emerge as critical determinants of activity. For oxadiazole-thioether antifungals, alterations at the R<sub>7</sub> position, such as *n*-pentyl or 4-methylbenzyl groups—correlate with enhanced inhibition of *Gibberella saubinetii*, *Sclerotinia sclerotiorum* and *Thanatephorus cucumeris*, indicating that optimal steric volume and lipophilicity at this position favour membrane interaction and/or target engagement (Section 3.6). In mandelic acid-piperazine hybrids, 3D-QSAR analysis around the R<sub>16</sub> substituent highlights how steric hindrance and electronic modulation on the piperazine ring govern antifungal potency against *Monilinia fructicola* by influencing both binding conformation and physicochemical properties (Section 3.7). Likewise, spirothiazolidinone-based antimycobacterial mandelic derivatives point to the importance of carefully selected aryl and heteroaryl substituents in achieving high inhibition of *Mycobacterium tuberculosis* H37Rv, likely by optimising multi-target engagement with enzymes such as HadAB, DprE1, Pks13, FadD32 and InhA (Section 3.7).

Heterocycle fusion onto the mandelic acid framework is another dominant design element. Phthalimide, pyrazole, thiazole, thiadiazole, oxadiazole, thiazolidinone and piperazine units each contribute distinct pharmacophoric features. For example, incorporation of the phthalimide ring enhances both antimicrobial and anti-inflammatory activity, probably by reinforcing  $\pi$ - $\pi$  stacking and improving target binding while hydrophobic mandelate substituents aid membrane permeation (Section 3.3). In contrast, pyrazole amide linkages deliver potent anti-TMV effects, where the pyrazole ring functions as a privileged antiviral pharmacophore and the mandelate ring electronics fine-tune potency (Section 3.4). Thiazole and thiadiazole hybrids designed as T3SS inhibitors reveal that subtle variation in benzyl substituents (e.g. 4-fluorobenzyl vs. 2-methylbenzyl) can switch and enhance anti-virulence profiles without impairing bacterial growth, emphasising that virulence-targeted SAR is highly sensitive to both electronic and steric features at the benzylic position (Section 3.7).

The 4-thiazolidinone ring provides an instructive example of non-classical SAR in enzyme inhibition. Thiazolidinone-based mandelic acid derivatives inhibit hCA IX without relying on a sulfonamide zinc-binding group, instead exploiting the thiazolidinone as a pharmacophore for isoform recognition and using aryl substituents on the mandelate ring to modulate lipophilicity and  $\pi$ -interactions within the active-site environment (Section 3.5). This demonstrates that mandelic acid can be successfully integrated into non-zinc-binding architectures to achieve potent and potentially safer hCA IX inhibition. The same heterocyclic core, when combined with mandelic acid and further decorated with appropriate aryl groups, yields anti-cancer hybrids with selective cytotoxicity towards melanoma cells, suggesting that subtle reorganisation of the same building blocks can redirect biological outcomes from enzyme inhibition to tumour cell killing (Section 3.7).

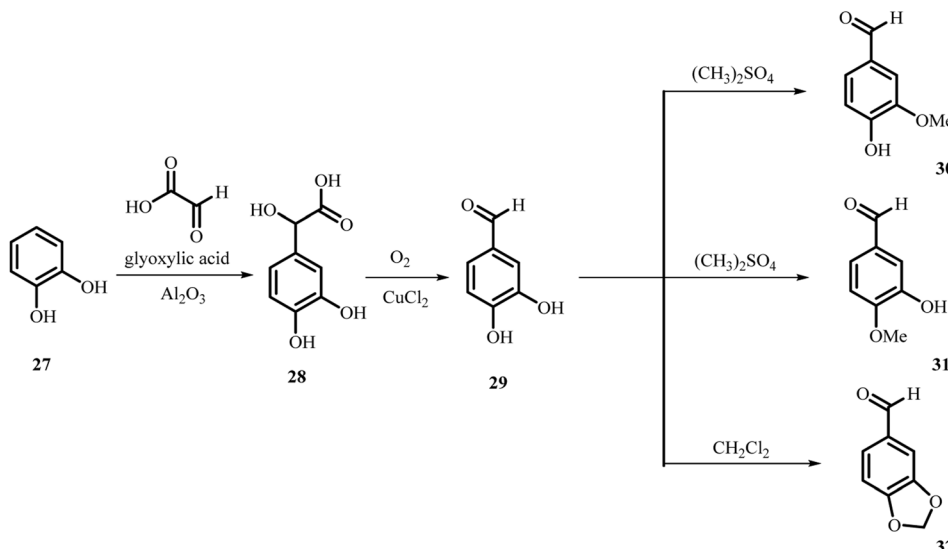
Stereochemical control adds an additional layer of SAR refinement. Chiral 1,3,4-oxadiazole-thioether mandelic derivatives reveal that *S*-configured analogues generally exhibit superior antifungal activity, indicating a stereoselective fit to fungal targets (Section 3.6). Likewise, the antiviral properties of poly(mandelic acid) derivatives (PMDA/SAMMA) depend not only on average molecular weight and degree of sulfonation but also on how the polymer microstructure—dictated by the synthetic route—presents chiral mandelate units and functional groups in three-dimensional space (Section 3.2). These observations highlight the need to consider chirality and higher-order structural organisation, especially when moving from small molecules to polymeric mandelic systems.

Mechanistic data further reinforce the SAR trends. Mandelic hybrids that disrupt fungal membranes and trigger ROS over-production (piperazine derivatives) connect increased lipophilicity and optimised steric profiles with membrane perturbation and downstream lipid peroxidation. In contrast, T3SS-targeting mandelic derivatives act in a non-bactericidal, virulence-suppressive manner, with gene-expression data (e.g. downregulation of *hryY* and *CsLOB1*) mapping directly onto the presence of specific benzyl substituents. hCA IX inhibitors exemplify how non-zinc-directed binding can be achieved through carefully oriented thiazolidinone and aryl mandelate components, re-emphasising that mandelic acid scaffolds are compatible with both classical and emerging inhibition paradigms.

Taken together, the SAR insights across anticoagulant, antiviral, anti-inflammatory, anti-virulence, antimycobacterial, antifungal and anticancer applications show that mandelic acid is not merely a convenient synthetic handle but a structurally rich and tunable core. By judicious selection of (i) aromatic ring substitution (electronic and steric), (ii) heterocyclic partner, (iii) stereochemical configuration and (iv) side-chain architecture, mandelic acid derivatives can be rationally engineered to access distinct targets and mechanisms with high precision. This convergence of SAR themes across disparate biological systems underscores the true biological promise of mandelic acid derivatives and provides a robust design framework for future therapeutic and agrochemical optimisation.

## 4 Mandelic acid derivatives possessing chemical applications

Mandelic acid derivatives are valuable intermediates in synthetic organic chemistry due to their aromatic ring and chiral  $\alpha$ -hydroxy acid functionality. This combination imparts high reactivity and selectivity, enabling their wide use in asymmetric synthesis, chiral resolution, and complex molecule construction. Their compatibility with transformations such as esterification, amidation, oxidation, and cyclization facilitates access to diverse fine chemicals, ligands, and catalysts. They also serve as important precursors for pharmaceuticals, agrochemicals, and specialty polymers. Continued investigation of their stereochemical features and functional group versatility drives the development of new synthetic methodologies, reinforcing the central role of mandelic acid derivatives in modern chemical synthesis.



**Scheme 4** Synthesis of vanillin (30), iso-vanillin (31), and heliotropin (32) from a mandelic acid derivative, adapted from ref. 104 with permission from [ACS] [Minisci *et al.*, 2000], copyright 2000.

#### 4.1. Selective oxidation and functionalization of mandelic acid derivatives: novel synthetic routes to vanillin, *iso*-vanillin, and heliotropin

Mandelic acid derivatives provide a convenient entry into several high-value aromatic aldehydes used in the flavour and fragrance industry. Minisci and co-workers (2000) demonstrated an elegant and scalable approach in which catechol (27) reacts with glyoxylic acid to form mandelic acid intermediates that undergo selective oxidative decarboxylation to yield protocatechualdehyde (29), vanillin (30), *iso*-vanillin (31), and heliotropin (32) (Scheme 4).<sup>104</sup> The distribution of products arises from the differing acidity of the two hydroxyl groups in catechol, which directs regioselective methylation.

This mandelate-based strategy provides a practical alternative to traditional *iso*-vanillin (31) synthesis, which historically required harsh reagents such as sodium hydride and methyl iodide in DMSO. In contrast, Minisci's method uses accessible starting materials, avoids expensive reagents, and is adaptable to industrial scale, highlighting how mandelic acid intermediates simplify oxidative and functionalization pathways in fine-chemical synthesis.

The oxidative conversion of 3,4-dihydroxymandelic acid (28) to protocatechualdehyde (29) proceeds *via* a Cu(II)-mediated catalytic cycle in which hydrogen peroxide assists in re-oxidizing Cu(I) back to Cu(II) (Scheme 5). The underlying transformation is mechanistically illustrated in Scheme 6.

However, oxidation using molecular oxygen in the presence of Cu(II) catalysts resulted in reduced yields of protocatechualdehyde (29), primarily due to the formation of significant amounts of a dimeric side product (33) *via* undesired dimerization pathways (Scheme 7).

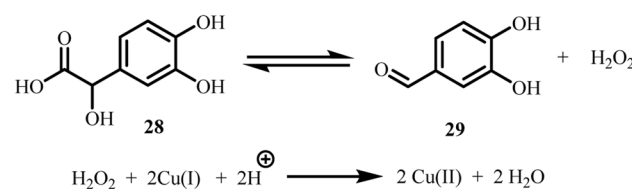
After discussing selective oxidation and functionalization strategies for mandelic acid derivatives leading to value added products such as vanillin, *iso*-vanillin, and heliotropin, the

focus now shifts to Bi<sup>0</sup> catalyzed oxidation, which offers remarkable substrate selectivity.

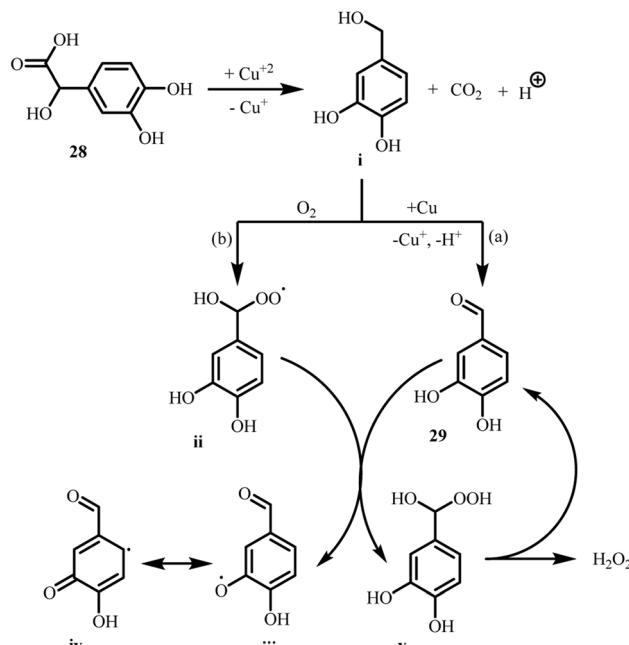
#### 4.2. Bi<sup>0</sup>-catalyzed oxidation of mandelic acid derivatives highlighting substrate selectivity

Bismuth-based catalytic systems offer an environmentally benign approach for the selective oxidation of mandelic acid derivatives. Duñach and co-workers (2002) reported a Bi<sup>0</sup>/DMSO/O<sub>2</sub> protocol that efficiently transforms mandelic acids into benzaldehydes or benzoic acids under mild conditions, the first catalytic oxidation system using Bi<sup>3+</sup> and molecular oxygen (Scheme 8).<sup>105</sup> This advance converted earlier stoichiometric Bi<sup>5+</sup>/Bi<sup>3+</sup> redox chemistry into a practical catalytic platform. The Bi<sup>0</sup>/DMSO/O<sub>2</sub> system also showed broad functional group tolerance, enabling oxidation of epoxides to  $\alpha$ -diketones and conversion of  $\alpha$ -hydroxy acids and  $\alpha$ -ketols to the corresponding carboxylic acids, underscoring its versatility.

The chemoselectivity of the oxidation strongly depended on the electronic and positional characteristics of aromatic substituents. Hydroxyl groups at the 2- or 4-positions favoured benzaldehyde formation, whereas electron-withdrawing substituents led to selective benzoic acid formation. The reaction proceeded efficiently in DMSO or DMF but was inactive in aqueous media, especially for unsubstituted mandelic acid. A mechanism involving formation of an  $\alpha$ -keto acid intermediate



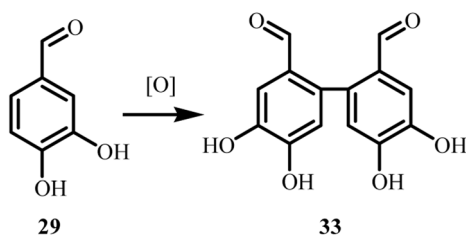
**Scheme 5** Oxidative conversion of compound 28 to compound 29 using a copper salt, adapted from ref. 104 with permission from [ACS] [Minisci *et al.*, 2000], copyright 2000.



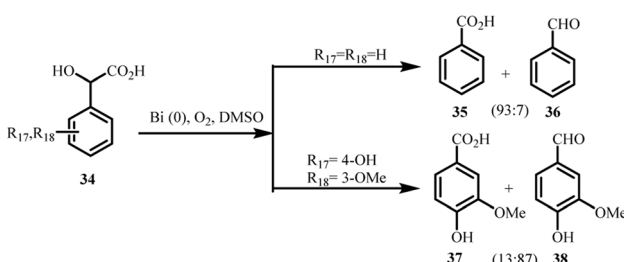
Scheme 6 Proposed Cu(II)-catalyzed oxidation mechanism, adapted from ref. 104 with permission from [ACS] [Minisci *et al.*, 2000], copyright 2000.

followed by oxidative cleavage has been proposed. Electron-donating substituents often produced mixed aldehyde–acid products due to competing pathways, thereby reducing overall selectivity.

Path 2 of Scheme 9 delineates an alternative oxidative pathway that proceeds through the formation of an  $\alpha$ -keto acid intermediate, ultimately facilitating the selective synthesis of carboxylic acid derivatives.



Scheme 7 Formation of the dimeric side product 33 during oxidation, adapted from ref. 104 with permission from [ACS] [Minisci *et al.*, 2000], copyright 2000.



Scheme 8 Substrate selectivity in Bi(0)-catalyzed oxidation of mandelic acid derivatives.<sup>105</sup>

The Bi<sup>0</sup>/DMSO/O<sub>2</sub> oxidative system exhibits remarkable chemo- and regioselectivity in transforming mandelic acid derivatives, with product outcomes strongly influenced by the electronic nature and position of aromatic substituents (Scheme 10).

Fluoro- and trifluoromethyl-substituted mandelic acids (entries 1–2) underwent highly selective oxidation to their corresponding carboxylic acids with excellent yields (97–99%) and minimal aldehyde formation (Table 1). Similarly, 3- and 4-chloromandelic acids (entries 3–4) showed >97% selectivity for acid formation. However, the 2-chloro analogue (entry 5) displayed reduced conversion (17%) and diminished selectivity (71 : 29), likely due to the steric hindrance from the *ortho*-substituent (“ortho effect”).

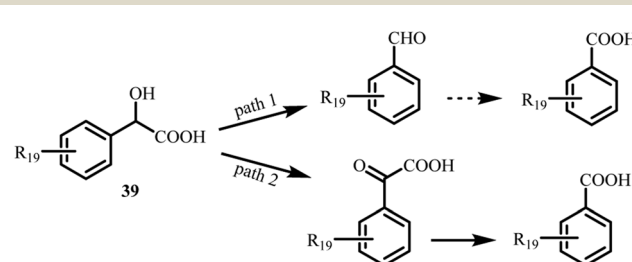
A shift in selectivity emerged for hydroxy-substituted mandelic acids (entries 6–14). While some derivatives showed moderate acid selectivity, those with hydroxyl groups at the 2- or 4-position (entries 9–11) predominantly yielded aldehydes with impressive selectivity (up to 99%) and full conversion in as little as 1 hour. These results point to the pivotal role of *ortho/para* hydroxyl groups in directing oxidation towards aldehydes, likely through electronic activation and hydrogen bonding.

In summary, this Bi<sup>0</sup>-catalyzed system offers a green and tunable oxidation protocol, allowing precise control over acid *vs.* aldehyde formation simply by adjusting the aromatic substitution pattern.

Building on the insights gained from Bi<sup>0</sup> catalyzed oxidation of mandelic acid derivatives and its notable substrate selectivity, the discussion now turns to Bi(0)/O<sub>2</sub> catalyzed oxidation, with particular emphasis on the underlying mechanistic aspects.

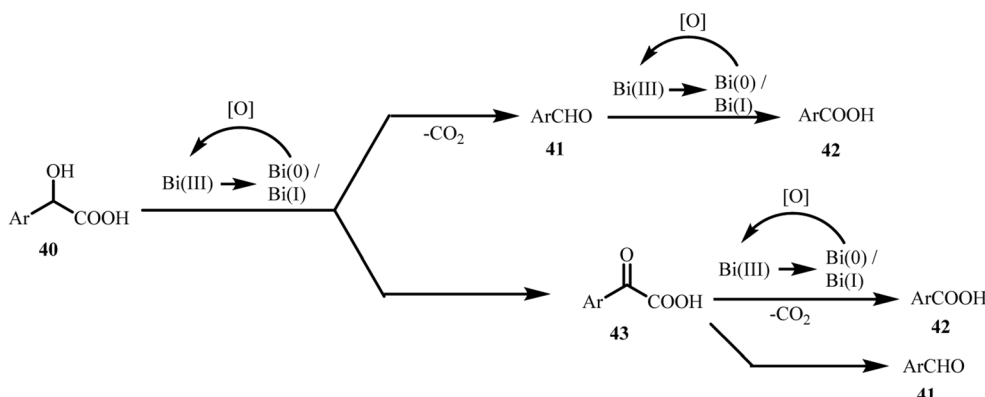
#### 4.3. Bi(0)/O<sub>2</sub>-catalyzed oxidation of mandelic acid derivatives and associated mechanistic considerations

Favier *et al.* (2003) expanded the understanding of bismuth-mediated oxidation by clarifying the mechanistic features of the Bi<sup>0</sup>/O<sub>2</sub> system previously reported by Duñach and co-workers.<sup>105,106</sup> This study employed stoichiometric amounts of bismuth-based reagents, such as sodium bismuthate and bismuth nitrate, to explore the chemoselective oxidation of various mandelic acid derivatives (40), arylaldehydes (41), and arylglyoxylic acids (43) (Scheme 10). By systematically examining different substitution patterns, the researchers aimed to delineate a plausible reaction mechanism and identify key



Scheme 9 Formation of aldehyde and  $\alpha$ -keto acid intermediates during the oxidation of mandelic acid derivatives.<sup>105</sup>



Scheme 10 Proposed pathways for  $\text{Bi}^0/\text{O}_2$ -catalyzed oxidation of mandelic acid derivatives.<sup>106</sup>

intermediates involved in the oxidation process. This work marked a significant step forward in the development of selective and sustainable oxidation protocols within the realm of bismuth chemistry.

The proposed mechanism revealed that the oxidation of mandelic acid derivatives was efficiently catalyzed by the  $\text{Bi}^0/\text{O}_2$  system in a DMSO/AcOH medium. The transformation proceeded *via* the initial formation of an  $\alpha$ -keto acid intermediate, followed by an oxidative decarboxylation step. During the process, elemental bismuth ( $\text{Bi}^0$ ) was oxidized to a  $\text{Bi}(\text{III})$  complex, with the  $\text{Bi}(\text{III})/\text{Bi}(\text{I})$  redox cycle mediating each oxidative event. Crucially, molecular oxygen acted as the terminal oxidant, regenerating  $\text{Bi}(\text{III})$  and sustaining the catalytic cycle (Scheme 11). This elegant redox interplay underscores the efficiency and sustainability of the  $\text{Bi}^0/\text{O}_2$  catalytic system.

A direct oxidative decarboxylation pathway was observed for specific substrates, leading predominantly to aldehyde formation, as illustrated in Scheme 12.

The catalytic cycle was most prominent with mandelic acid derivatives bearing hydroxyl substituents at the 2- or 4-positions of the aromatic ring. The proposed mechanism further implicated the formation of quinoid-type intermediates as key species driving the oxidative transformation (Scheme 13).

The nature and position of substituents on the aromatic ring exert a significant chemoselective influence on the outcome of the  $\text{Bi}(0)/\text{O}_2$ -catalyzed oxidation of mandelic acid derivatives, as illustrated in Scheme 14 and summarized in Table 2.

The  $\text{Bi}^0/\text{O}_2$ -catalyzed oxidation of mandelic acid derivatives showed strong chemoselectivity, significantly influenced by the nature and position of substituents on the aromatic ring. As shown in Table 2, the parent mandelic acid (entry 1,  $\text{R}_{21} = \text{H}$ ,  $\text{R}_{22} = \text{H}$ ) gave moderate conversion (54%) and favoured carboxylic acid formation with a 7:93 aldehyde-to-acid ratio. Introduction of an electron-donating methoxy group (entry 2,  $\text{R}_{21} = \text{OMe}$ ) accelerated the reaction (77% conversion in 6 h) and increased aldehyde formation (38:62 ratio). In contrast, an electron-withdrawing trifluoromethyl group (entry 3,  $\text{R}_{21} = \text{CF}_3$ ) led to near-complete selectivity for the acid product (1:99), highlighting the impact of electronic effects.

Notably, hydroxy-substituted derivatives (entries 4 and 5) displayed fast reaction rates and high aldehyde selectivity. For

example, the 4-hydroxy-3-methoxy derivative (entry 4) achieved 97% conversion in just 40 minutes with an aldehyde-to-acid ratio of 87:13. Similarly, the 4-hydroxy derivative (Entry 5) delivered 100% conversion in 6 hours, predominantly yielding the aldehyde (77:23).

These results underline the critical role of electron-donating groups, especially hydroxyl substituents in the *ortho* or *para* positions, in steering the oxidation towards selective aldehyde formation under  $\text{Bi}^0/\text{O}_2$  catalysis.

Observations revealed a clear substituent-dependent selectivity in the  $\text{Bi}^0/\text{O}_2$ -catalyzed oxidation of mandelic acid derivatives. Specifically, electron-donating groups (EDGs), particularly hydroxyl groups at the 2- and/or 4-positions of the aromatic ring—favoured the formation of aldehydes. This pathway likely proceeds through quinoid-type intermediates. Conversely, electron-withdrawing groups (EWGs) led the reaction toward carboxylic acid formation *via* oxidative decarboxylation of the corresponding  $\alpha$ -keto acid intermediates. Moreover, EWGs were found to slow down the reaction, highlighting the sensitivity of the process to electronic effects.

#### 4.4. Chiral dopants derived from optically active *p*-substituted mandelic acids

Optically active *p*-substituted mandelic acids provide a versatile platform for designing chiral dopants capable of inducing helical ordering in achiral liquid-crystalline materials. Lesac *et al.* (2003) developed a series of mandelic acid esters (**50** and **51**) prepared from enantiomerically pure *p*-substituted mandelic acids (Fig. 11), demonstrating that subtle modifications in substituent type and chain length strongly influence molecular self-assembly and mesophase behaviour.<sup>107</sup> Among these, *p*-hydroxymandelic acid derivatives were particularly valuable because the hydroxy and carboxylate groups allow extension of the aromatic core or attachment of flexible alkyl chains, enabling fine control over dopant geometry. The position and nature of substituents on the mandelate ring, along with the length and flexibility of appended alkyl chains, directly modulate the chiral induction ability of the dopants by controlling molecular shape and packing.

The racemic precursors, 4-decyloxymandelic acid (**53**) and 4-benzylloxymandelic acid (**54**), were prepared *via* the insertion of

Table 1 Substrate scope in Bi<sup>0</sup> catalyzed oxidation reaction.<sup>105</sup>

Entry	Substrate	Time	Conversion (%)	Yield (%)	Acid to aldehyde ratio
1		24 h	72	97	97 : 3
2		24 h	97	99	99 : 1
3		24 h	56	98	98 : 2
4		24 h	95	> 98	97 : 3
5		24 h	17	> 98	71 : 29
6		61 h	77	> 98	62 : 38
7		24 h	40	> 98	85 : 15
8		24 h	17	> 98	65 : 35
9		6 h	100	> 98	23 : 77

Table 1 (Contd.)

Entry	Substrate	Time	Conversion (%)	Yield (%)	Acid to aldehyde ratio
10		8 h	100	80	5 : 95
11		1 h	100	38	1 : 99
12		3 h	41	50	81 : 19
13		1 h	94	> 98	6 : 94
14		4 h	82	> 98	22 : 78

chlorocarbene into *p*-substituted benzaldehydes (52), affording moderate yields ranging from 40% to 70% (Scheme 15). In this transformation, benzyltriethylammonium chloride (BTAC) functioned as a phase-transfer catalyst, facilitating the *in situ* generation of dichlorocarbene from chloroform under strongly basic conditions. This method enabled efficient construction of the desired mandelic acid framework, serving as a crucial step toward the development of chiral dopants for liquid crystalline applications.

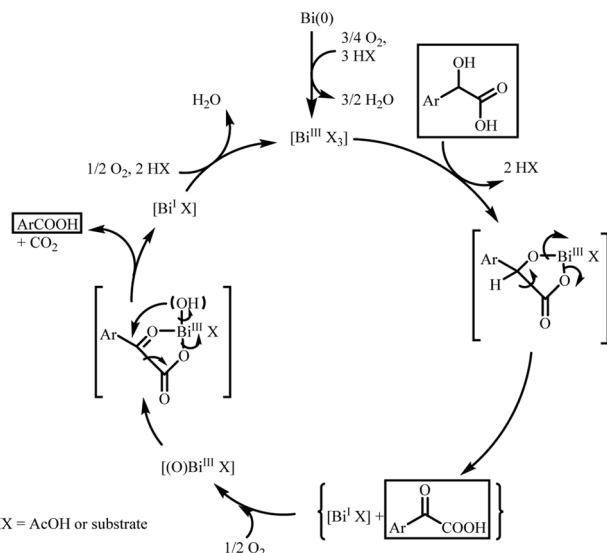
The convergent synthesis of mandelate (+)-50 required the independent preparation of the phenolic ester precursor 63, which played a key role in the subsequent esterification of optically active mandelic acid (+)-55 (Scheme 16). To obtain compound 63, phenol 61 was coupled with 4-OTHP-protected benzoic acid 62 in tetrahydrofuran (THF) using dicyclohexylcarbodiimide (DCC) as a coupling agent and 4-dimethylaminopyridine (DMAP) as a catalyst, affording the protected ester intermediate in approximately 74% yield. The protecting group was then cleanly removed using pyridinium *p*-

toluenesulfonate (PPTS) under mild acidic conditions in wet acetone, giving access to the free phenol derivative 63 in excellent purity, ready for esterification with (+)-55.

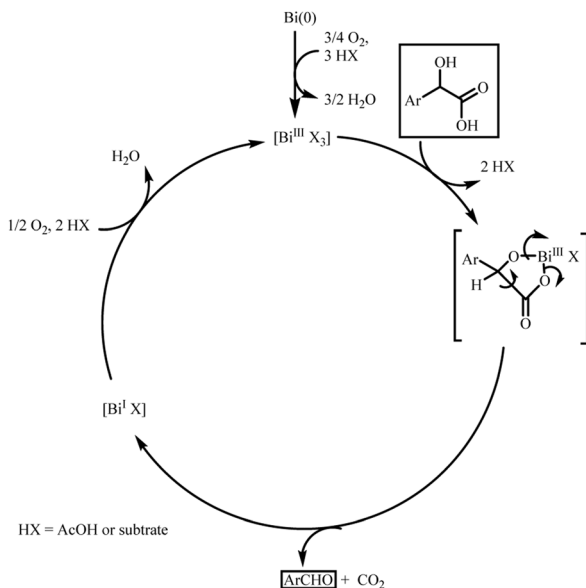
Furthermore, ester (+)-65, incorporating a polar stereogenic centre within a rigid aromatic core, was synthesized through the esterification of OTHP-protected mandelic acid (+)-55 with alcohol 63. Subsequent acid-catalyzed deprotection using pyridinium *p*-toluenesulfonate (PPTS) in wet acetone afforded the target ester (+)-65 in approximately 25% yield, while retaining a remarkable enantiomeric excess (ee) of 99%. This high enantiomeric purity closely matched that of the starting material, decyloxymandelic acid, confirming the stereochemical integrity of the transformation (Scheme 17).

To strategically position the stereogenic centre at the periphery of the rigid molecular core in compound (+)-69, a long alkyl chain was introduced at the carboxylic terminus of (+)-56. This was achieved through a DCC-mediated esterification of OTHP-protected chiral benzyloxymandelic acid with 1-dodecanol. The resulting intermediate underwent hydrogenolysis to





Scheme 11 Proposed catalytic cycle for the formation of benzoic acids via  $\text{Bi}^0/\text{O}_2$  oxidation.<sup>106</sup>



Scheme 12 Proposed catalytic cycle for the formation of benzaldehydes via oxidative decarboxylation.<sup>106</sup>

remove the benzyl protecting group, affording compound 67. Subsequent acylation with 4-dodecyloxybiphenyl carboxylic acid, followed by mild acid hydrolysis to remove the OTHP group, furnished the target ester (+)-69 with an enantiomeric excess of 99% and an overall yield of approximately 20% (Scheme 18).

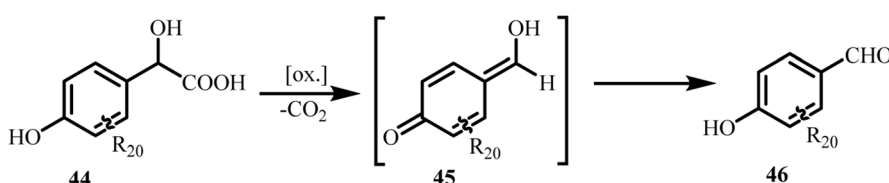
Mandelic acid derivatives are important intermediates for the industrial synthesis of aromatic aldehydes used in flavour and fragrance formulations. Hydroxy- and alkoxy-substituted aldehydes such as vanillin (30) and piperonal (32) are commonly obtained by oxidising their corresponding mandelic acid precursors, including 4-hydroxy-3-methoxymandelic acid (70) and 3,4-methylenedioxymandelic acid (71) (Scheme 19). These aldehydes also serve as key intermediates in pharmaceutical, agrochemical, and cosmetic products, reflecting the broad synthetic value of mandelic acid-based transformations. Metal-catalysed oxidations of mandelic acid derivatives using molecular oxygen ( $\text{O}_2$ ) can yield divergent outcomes depending on the catalyst:  $\text{Cu}(\text{II})$ ,  $\text{Pd/C}$ , and  $\text{Pt/C}$  typically favour aryl-glyoxylic acids, whereas  $\text{Ce}(\text{IV})$ ,  $\text{Mn}(\text{II})/\text{Br}^-$ ,  $\text{Ru}(\text{VI})/\text{Fe}(\text{III})$ , and  $\text{Co}(\text{III})/\text{O}_2$  systems promote full oxidation to benzoic acids. Such controllable oxidation pathways highlight the versatility and commercial relevance of mandelic acid-derived products.

#### 4.5. New chiral ligands from mandelic acid for asymmetric phenyl transfer to aromatic aldehydes

In addition to their role in oxidation chemistry, (*R*)- and (*S*)-mandelic acids, readily available and inexpensive chiral building blocks have found wide application in the synthesis of  $\alpha$ -hydroxy-2-oxazolines, which are valuable heterocycles in asymmetric catalysis. In 2004, Bolm and co-workers developed an efficient protocol for synthesizing oxazoline ring (75), starting from enantiomerically pure mandelic acid derivatives. The method involved condensation of  $\beta$ -amino alcohols with mandelic acid-derived acid chlorides (72), followed by intramolecular cyclization (Scheme 20).<sup>108</sup> The resulting chiral oxazolines functioned as ligands in asymmetric phenyl transfer reactions, delivering good yields (up to 76%) with moderate enantioselectivity (35%), showcasing the potential of mandelic acid scaffolds in enantioselective transformations.

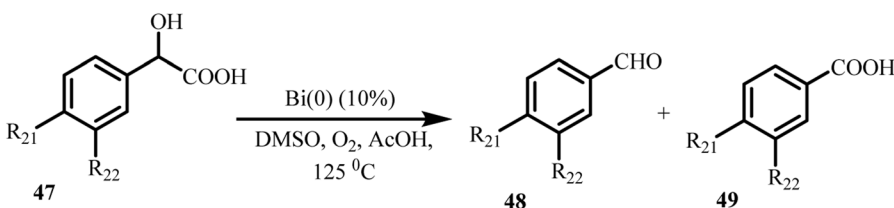
#### 4.6. Highly diastereoselective arylation of (*S*)-mandelic acid enolate leading to enantioselective synthesis of substituted (*R*)-3-hydroxy-3-phenyloxindoles, (*R*)-benzylic acids and nitrobenzophenones

In 2004, Barroso *et al.* employed a versatile route to structurally diverse enantiomerically pure (*R*)-3-hydroxy-3-phenyloxindoles, and (*R*)-benzylic acids.<sup>109</sup> Notably, the study also demonstrated that aerobic oxidative decarboxylation of chiral benzylic acids offers a practical and green approach for constructing substituted benzophenone frameworks, which are valuable scaffolds in medicinal and materials chemistry.

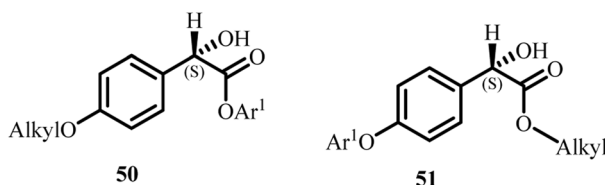


Scheme 13 Proposed quinoid-type intermediate involved in the oxidation process.<sup>106</sup>



Scheme 14  $\text{Bi}^0/\text{O}_2$ -catalyzed oxidation of mandelic acid derivatives.<sup>106</sup>Table 2 Substrate scope for  $\text{Bi}^0/\text{O}_2$  catalyzed oxidation of mandelic acid derivatives.<sup>106</sup>

Entry	$\text{R}_{21}$	$\text{R}_{22}$	Conversion (%)	Yield (%)	Aldehyde to acid ratio
1	H	H	54	81 <sup>a</sup>	7:93
2 <sup>b</sup>	OMe	H	77	100	38:62
3	CF <sub>3</sub>	H	97	100	1:99
4 <sup>c</sup>	OH	OMe	97	100	87:13
5 <sup>b</sup>	OH	H	100	98	77:23

<sup>a</sup> Phenylglyoxylic acid was formed in 19% yield. <sup>b</sup> Reaction time 6 hours.<sup>c</sup> Reaction time 40 minutes.Fig. 11 Representative esters derived from enantiomerically pure *p*-substituted mandelic acids.<sup>107</sup>

The synthesis of (*R*)-3-hydroxy-3-phenyloxindoles (**80**) took place *via* diastereoselective arylation of the lithium enolate generated from a (*S,S*)-*cis*-1,3-dioxolan-4-one (**77**), itself derived from optically active (*S*)-mandelic acid (**76**), using *o*- or *p*-halonitrobenzene electrophiles (**78**) (Scheme 21).<sup>109</sup> These arylation reactions proceed smoothly, furnishing the corresponding products in high yields with excellent diastereoselective control. Subsequent Zn/HCl/EtOH-mediated reduction of the nitro group in the *ortho*-substituted adducts triggered an intramolecular aminolysis of the dioxolanone ring, directly affording enantiopure (*R*)-3-hydroxy-3-phenyloxindoles (**80**).

Compound **85** was isolated as a by-product in 40% yield and was proposed to arise from an aldol reaction between the 1,3-

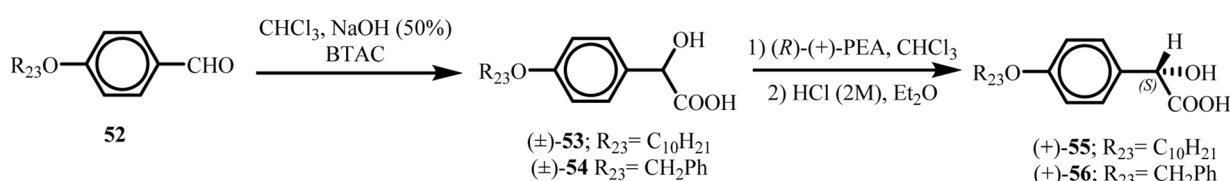
dioxolan-4-one enolate (**84**) and pivalaldehyde. Interestingly, the formation of **85** was exclusively observed in the presence of nitrobenzene, suggesting that the process involved a redox transformation (Scheme 22). This indicates a dual role of nitrobenzene, not only as a reactant but also as a redox mediator influencing the reaction pathway and by-product formation.

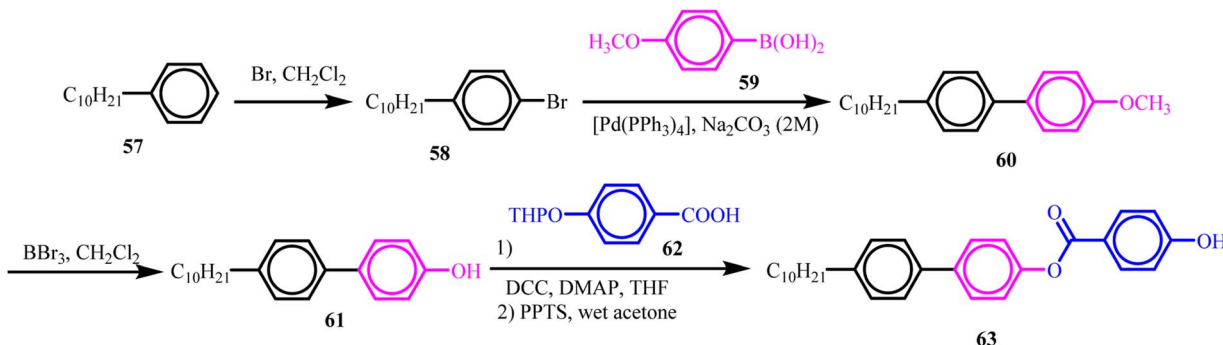
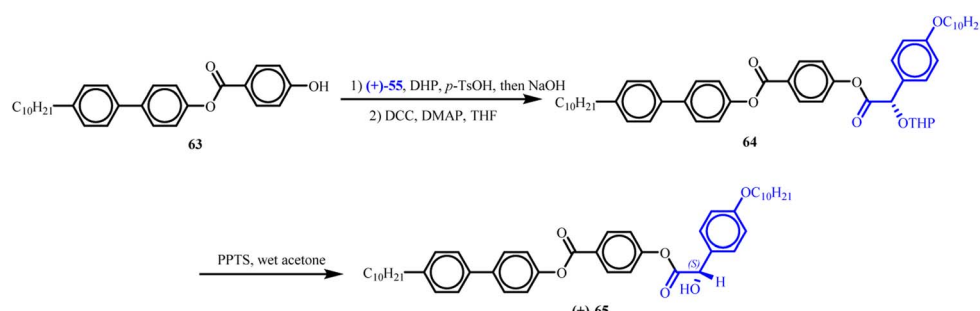
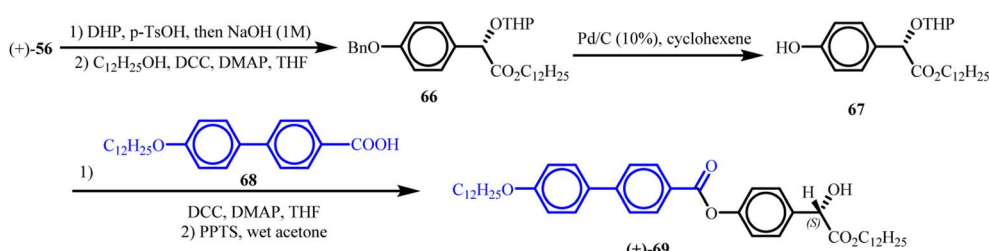
In contrast, basic hydrolysis of the protecting dioxolanone unit (**86**) (structurally analogous to compound **79**), applicable to both *ortho*- and *para*-arylated products, provides access to enantiomerically pure substituted (*R*)-benzylic acids (**87**) (Scheme 23). Further oxidative decarboxylation of these acids, using molecular oxygen as the terminal oxidant in the presence of pivalaldehyde and a Co(II)-Me<sub>2</sub>opba catalyst (**89**) (Fig. 12), yields the corresponding substituted nitrobenzophenones (**88**). This transformation highlights the efficiency of cobalt-catalyzed oxidation in accessing valuable aromatic ketone frameworks from mandelic acid-derived precursors.

Following the discussion on highly diastereoselective arylation of (*S*)-mandelic acid enolate for the enantioselective synthesis of diverse bioactive scaffolds, the focus now shifts to its application in the enantioselective synthesis of 2-substituted 1,4 diketones from (*S*)-mandelic acid enolate and  $\alpha,\beta$ -enones.

#### 4.7. Enantioselective synthesis of 2-substituted-1,4-diketones from (*S*)-mandelic acid enolate and $\alpha,\beta$ -enones

In 2006, Blay *et al.* reported a concise and efficient stereoselective method for the enantioselective synthesis of chiral 2-substituted-1,4-diketones (**93**) using (*S*)-mandelic acid (**76**) as the chiral precursor (Scheme 24).<sup>110</sup> These diketones are valuable intermediates for constructing biologically relevant scaffolds such as jasmones, cuparenones, prostaglandins, and other complex heterocyclic compounds. In this method, the lithium enolate generated from a 1,3-dioxolan-4-one (**77**), prepared from optically pure (*S*)-mandelic acid (**76**) and pivalaldehyde, undergoes smooth Michael addition to a range of  $\alpha,\beta$ -unsaturated carbonyl compounds, affording the corresponding

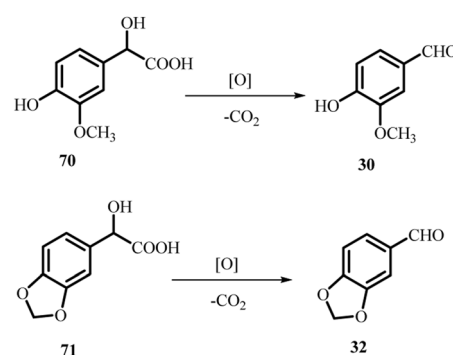
Scheme 15 Synthetic route for the preparation of intermediates (+)-55 and (+)-56.<sup>107</sup>

Scheme 16 Synthetic route for the preparation of intermediate 63.<sup>107</sup>Scheme 17 Synthetic route for the preparation of (+)-65.<sup>107</sup>Scheme 18 Synthetic route for the preparation of (+)-69.<sup>107</sup>

adducts in high yields with excellent diastereorecontrol. Subsequent basic hydrolysis of the dioxolanone protecting group (90) provides the corresponding  $\alpha$ -hydroxy acids (as hemiacetals) (92). These intermediates undergo oxidative decarboxylation, using molecular oxygen alongside pivalaldehyde and a Co(III)-Me<sub>2</sub>opba catalyst (89), to deliver optically enriched 2-substituted 1,4-dicarbonyl compounds (93) in very high enantiomeric purities. Interestingly, HMPA (hexamethylphosphoramide) played a crucial role in reversing and enhancing diastereoselectivity, effectively modulating the coordination environment of lithium and suppressing its catalytic role. This work elegantly demonstrated the utility of (S)-mandelic acid as an Umpolung chiral equivalent of the benzoyl anion in enabling highly stereocontrolled carbon–carbon bond construction and asymmetric synthesis.

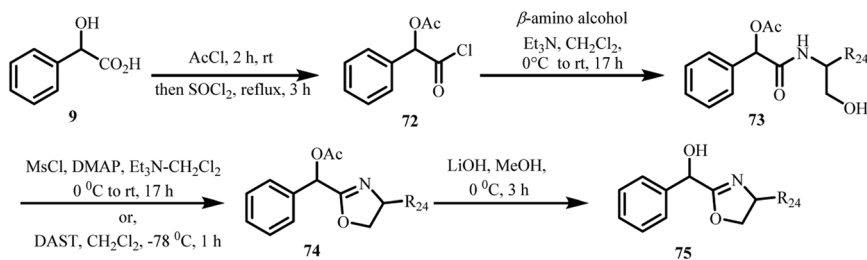
The reaction is postulated to proceed *via* an eight-membered chelated transition state, designated as TS-C and TS-E in the absence of HMPA (Fig. 13). In these chelated manifolds, Li<sup>+</sup> ions

serve as bidentate Lewis acids, simultaneously coordinating to the carbonyl oxygens of the enolate and the enone. This dual coordination enforces a rigid, cyclic transition state geometry, thereby lowering the activation barrier by stabilizing the

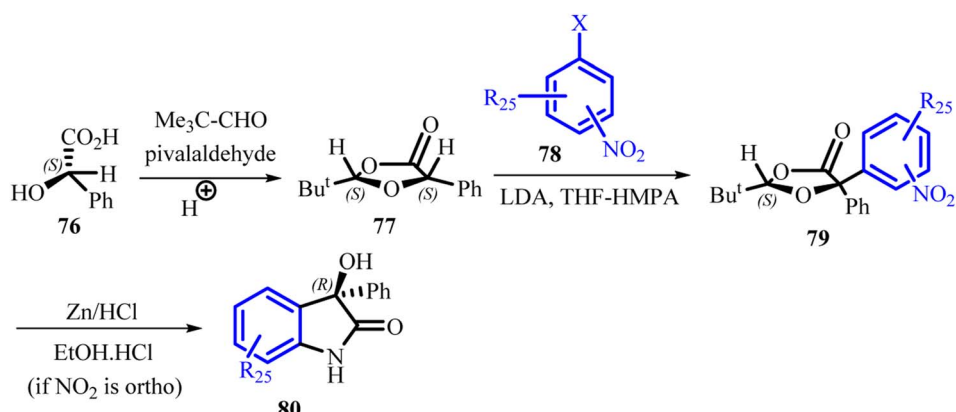


Scheme 19 Metal-catalyzed oxidation of mandelic acid derivatives.

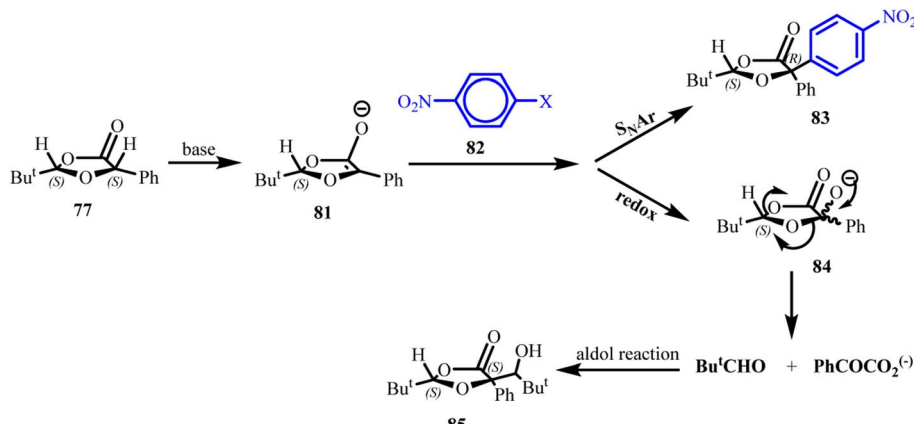




Scheme 20 Synthesis of oxazoline compound 75 via coupling of enantiopure mandelic acids with enantiopure  $\beta$ -amino alcohols.<sup>108</sup>



Scheme 21 Synthetic route for the preparation of (R)-3-hydroxy-3-phenyloxindoles, adapted from ref. 109 with permission from [ACS] [Barroso et al., 2004], copyright 2004.



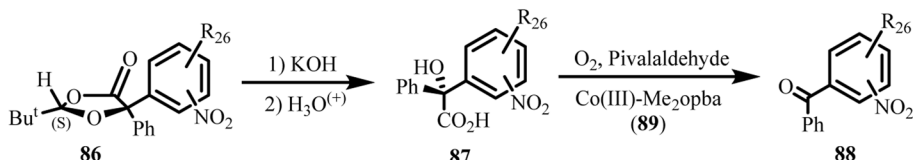
Scheme 22 Synthetic route for the formation of side product 85, adapted from ref. 109 with permission from [ACS] [Barroso et al., 2004], copyright 2004.

developing negative charge on the oxygen atoms. Between the two possibilities, TS-C is energetically favoured because its arrangement alleviates 1,3-diaxial-type steric repulsion between the bulky dioxolanone moiety and the benzoyl substituent, while also preserving optimal  $\pi$ -orbital overlap for C-C bond formation.

Upon introduction of HMPA, a strongly Lewis basic, aprotic additive, this chelation is effectively disrupted due to preferential solvation of  $\text{Li}^+$ , which competes with and displaces carbonyl coordination. This shifts the mechanism towards

a non-chelated transition state (TS-D), wherein  $\text{Li}^+$  exists predominantly as a solvent-separated ion pair. The geometry of TS-D minimizes gauche interactions between substituents on the reacting enolate and enone, but it no longer benefits from the enthalpic stabilization conferred by Li-O chelation.

Under the assumption that Curtin–Hammett kinetics govern the outcome, the reaction proceeds through a dynamic equilibrium between these chelated contact ion pair pathways (TS-C/E) and the non-chelated solvent-separated pathway (TS-D). The latter pathway, although potentially faster at low reactant



Scheme 23 Hydrolysis and Co(III)-catalyzed oxidative decarboxylation route for the synthesis of compound 88, adapted from ref. 109 with permission from [ACS] [Barroso *et al.*, 2004], copyright 2004.

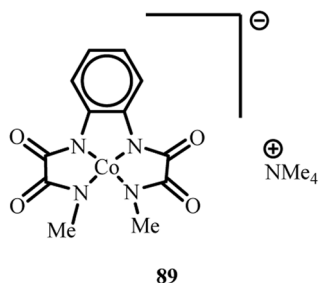


Fig. 12 Representative structure of the Co(III) *ortho*-phenylene-bis(*N*'-methoxy-amide) complex, adapted from ref. 109 with permission from [ACS] [Barroso *et al.*, 2004], copyright 2004.

concentrations due to reduced steric encumbrance, sacrifices stereochemical fidelity because the conformational constraints of the chelated manifold are absent. This mechanistic balance rationalizes the experimentally observed reduction in diastereoselectivity when HMPA is present, underscoring the critical role of  $\text{Li}^+$ -mediated organization of the reactive complex in steering stereoselectivity.

After examining the use of (*S*)-mandelic acid enolate in the enantioselective synthesis of 2-substituted 1,4-diketones from  $\alpha,\beta$ -enones, the discussion now turns to its role as a benzoyl anion equivalent for the enantioselective synthesis of non-symmetrical benzoinos.

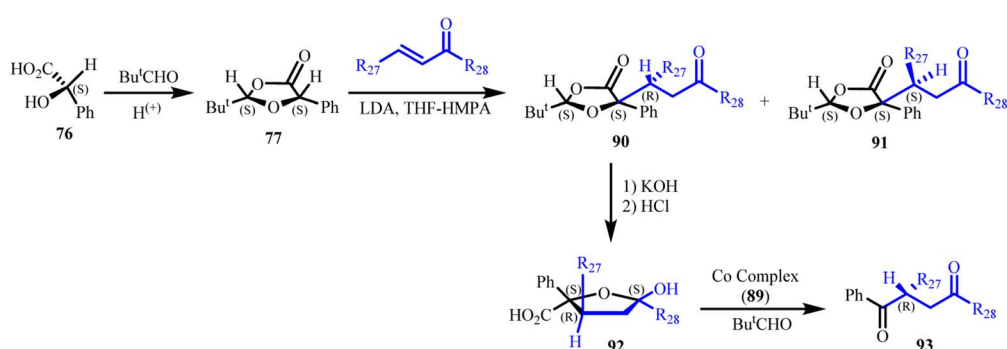
#### 4.8. Chiral (*S*)-mandelic acid enolate as a benzoyl anion equivalent for enantioselective synthesis of non-symmetrical benzoinos

In 2011, Blay *et al.* reported a detailed mechanistic study on the enantioselective synthesis of non-symmetrical substituted benzoinos starting from (*S*)-mandelic acid and various aromatic

aldehydes (Scheme 25).<sup>111</sup> The key intermediate was the lithium enolate of (*2S,5S*)-1,3-dioxolan-4-one (77), generated *in situ* from (*S*)-mandelic acid and pivalaldehyde, which underwent a highly diastereoselective aldol reaction products (94) with the aldehydes. The sequence continued with protection of the resulting hydroxyl group as 2-Methoxyethoxymethyl (MEM) ethers (95), and base-mediated hydrolysis of the dioxolanone ring (96). The resulting  $\alpha$ -hydroxy acid intermediates undergo oxidative decarboxylation (97), and subsequent deprotection of the MEM groups afforded the desired chiral, non-symmetrically substituted benzoinos (98), each obtained with excellent enantiomeric purity, showcasing both synthetic elegance and high stereochemical control in accessing complex chiral building blocks from simple optically active precursors. This sequence effectively positions (*S*)-mandelic acid as a versatile chiral benzoyl anion equivalent, enabling stereocontrolled access to structurally diverse benzoin derivatives.

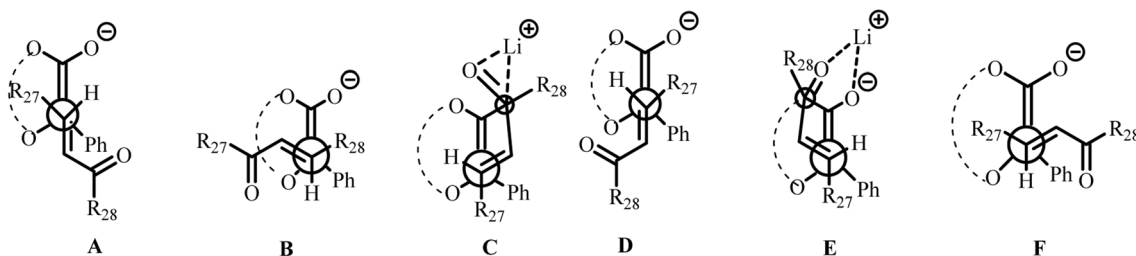
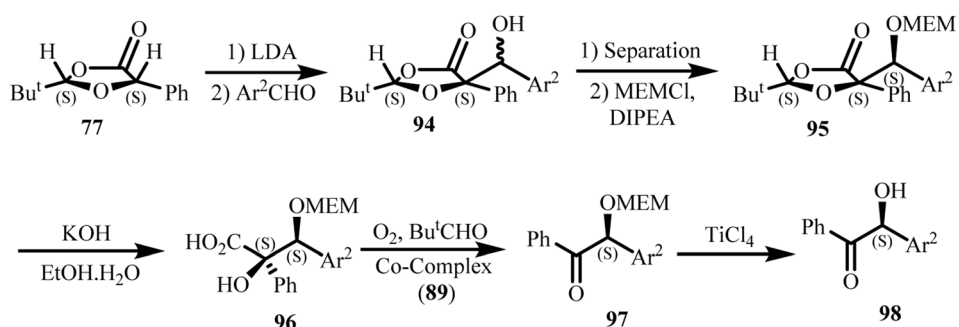
A comprehensive mechanistic investigation was undertaken to support the proposed reaction pathway and intermediates involved in the synthesis (Scheme 26). The researchers drew parallels to transition states previously proposed by Battaglia for a related reaction, specifically, the addition of the enolate of *cis*-1,3-dioxolan-4-one (derived from (*S*)-lactic acid and pivalaldehyde) to aldehydes, which offered a strong framework to explain the observed diastereoselectivity.

According to Seebach's principle of self-regeneration of stereocenters, also known as the Seebach product rule, the diastereomers 99 and 100 are formed *via* kinetically favoured transition states TS I and TS II, where the aldehyde approaches the Re face of the enolate, minimizing steric hindrance. In contrast, transition states TS III and TS IV represent an approach from the Si face, resulting in the formation of diastereomers 101 and 102, referred to as non-Seebach products.



Scheme 24 Synthesis of enantiopure 1,4-diketones (93).<sup>110</sup>



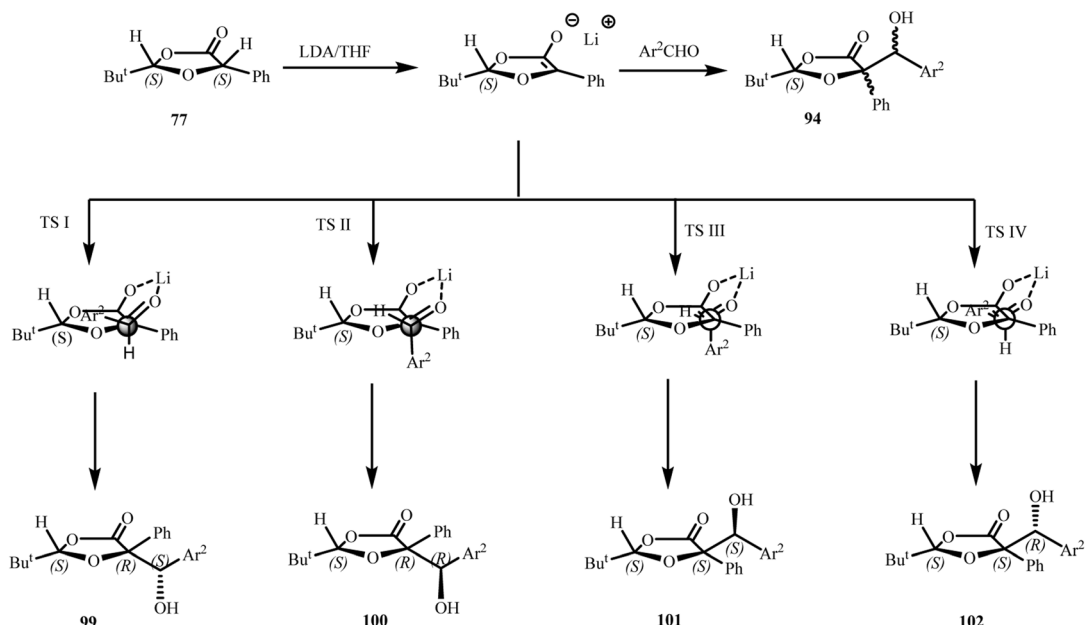
Fig. 13 Proposed transition state models for the reaction.<sup>110</sup>Scheme 25 Synthesis of non-symmetrically substituted chiral benzoins.<sup>111</sup>

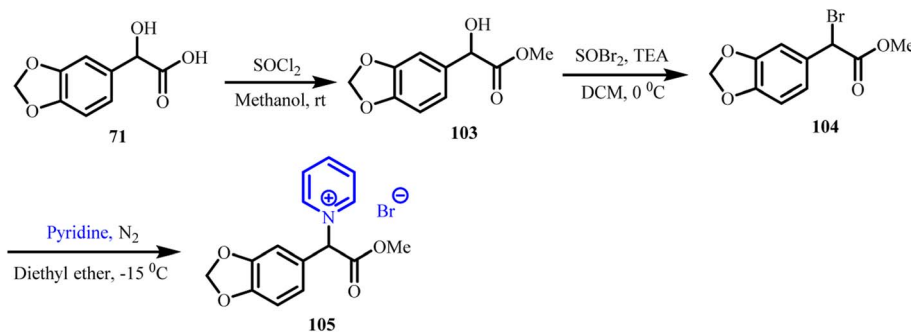
This stereochemical model elegantly explains the facial selectivity and product distribution observed in the studied transformation.

Concluding the discussion on the application of chiral (*S*)-mandelic acid enolate as a benzoyl anion equivalent for the enantioselective synthesis of non-symmetrical benzoins, the focus now moves to the synthesis and biological evaluation of imidazolium and pyridinium ionic liquids derived from mandelic acid.

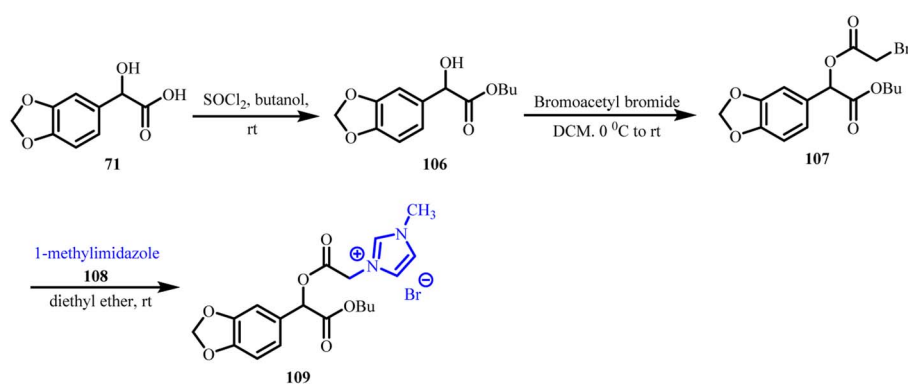
#### 4.9. Synthesis and biological assessment of imidazolium and pyridinium ionic liquids derived from mandelic acid

In 2013, Gathergood *et al.* reported the synthesis of imidazolium and pyridinium halide ionic liquids (ILs) derived from substituted mandelic acid derivatives, with a strong focus on environmental safety and sustainability.<sup>112</sup> These ILs exhibited remarkably low toxicity toward both bacteria and algae, addressing one of the key concerns in the development of truly “green” solvents. While ILs are often celebrated for their low

Scheme 26 Proposed transition state for the formation of the product.<sup>111</sup>



**Scheme 27** Synthetic route to ionic liquids featuring a heterocyclic nitrogen linked to a benzylic carbon, adapted from ref. 112 with permission from [ACS] [Gathergood *et al.*, 2013], copyright 2013.



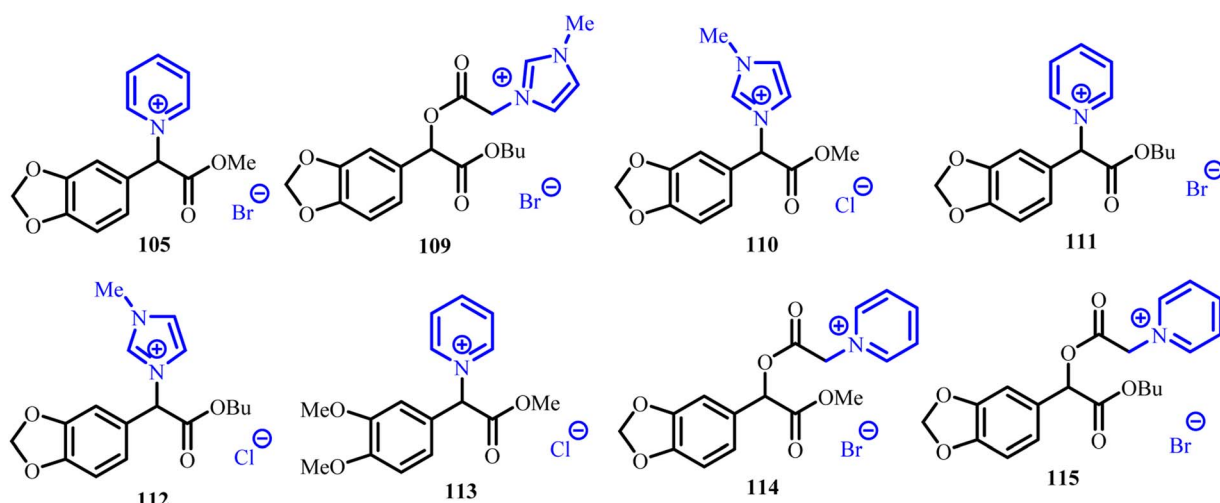
**Scheme 28** Synthetic route to ionic liquids featuring an acetoxy bridge between the benzylic carbon and the nitrogen of a pyridinium or methylimidazolium ring, adapted from ref. 112 with permission from [ACS] [Gathergood *et al.*, 2013], copyright 2013.

vapor pressure, non-flammability, and thermal stability, their increasing lipophilicity has been correlated with elevated toxicity in various ecosystems.

To ensure environmental compliance and safety, all synthesized ILs in the study were rigorously evaluated under the REACH regulatory framework (Registration, Evaluation, Authorization, and Restriction of Chemicals). The study

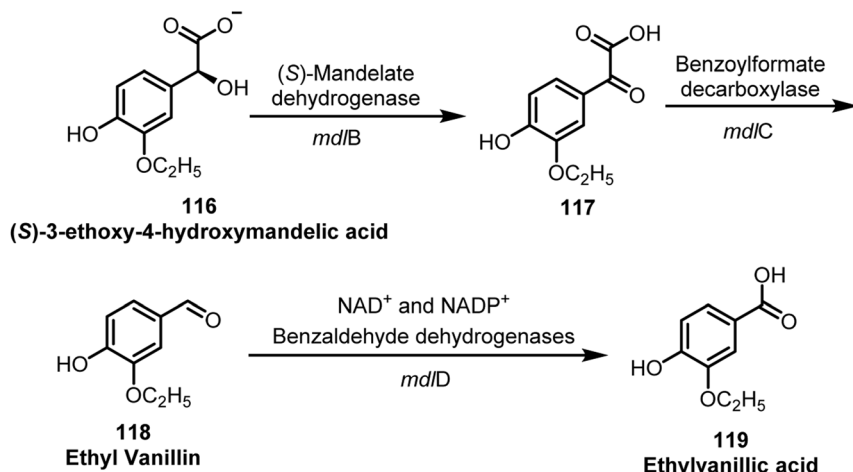
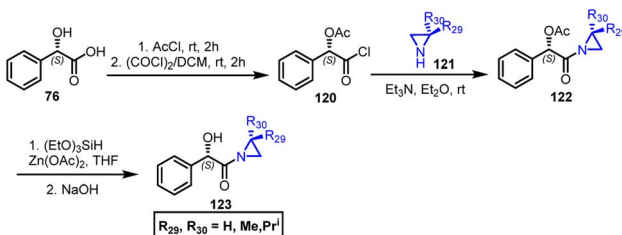
successfully introduced two structurally distinct classes of ionic liquids (Schemes 27 and 28), highlighting a promising route toward the development of low-toxicity, mandelic acid-based ILs for future green chemistry applications.

A diverse series of compounds is depicted in Fig. 14, categorized into two structural classes. The first group (compounds 105, 110–113) features a direct linkage between the nitrogen atom of



**Fig. 14** Representative structures of ionic liquids featuring (105, 110–113) a heterocyclic nitrogen linked to a benzylic carbon, and (109, 114–115) an acetoxy bridge between the benzylic carbon and the nitrogen of a pyridinium or methylimidazolium ring, adapted from ref. 112 with permission from [ACS] [Gathergood *et al.*, 2013], copyright 2013.



Scheme 29 Synthesis of ethyl vanillin via a single microbial fermentation process.<sup>116</sup>Scheme 30 Synthesis of mandelic acid-derived chiral ligand 123.<sup>123</sup>

a heterocyclic moiety and a benzylic carbon. In contrast, the second group (compounds 109, 114 and 115) incorporates an acetoxy bridge, connecting the benzylic carbon to the nitrogen atom of either a pyridinium or methylimidazolium ring.

Following the synthesis and biological assessment of imidazolium and pyridinium ionic liquids derived from mandelic acid, attention is now directed to the oxidative decarboxylation of mandelic acid derivatives by recombinant *Escherichia coli* as an innovative route for the synthesis of ethyl vanillin.

#### 4.10. Oxidative decarboxylation of mandelic acid derivatives by recombinant *Escherichia coli* as a novel approach to ethyl vanillin synthesis

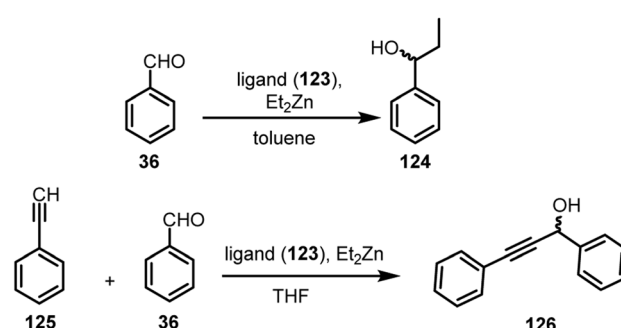
In the quest for a superior alternative to vanillin in the food and fragrance industries, ethyl vanillin (3-ethoxy-4-hydroxybenzaldehyde) (118) has emerged as a promising candidate due to its stronger aroma and greater stability during long-term storage and transport.<sup>113</sup> However, traditional methods for synthesizing ethyl vanillin *via* chemical catalysis raise concerns about safety, cost, and environmental impact due to the generation of hazardous by-products. In contrast, biotechnological approaches, particularly enzyme-catalyzed processes, offer a greener, safer, and more economical route.<sup>114</sup>

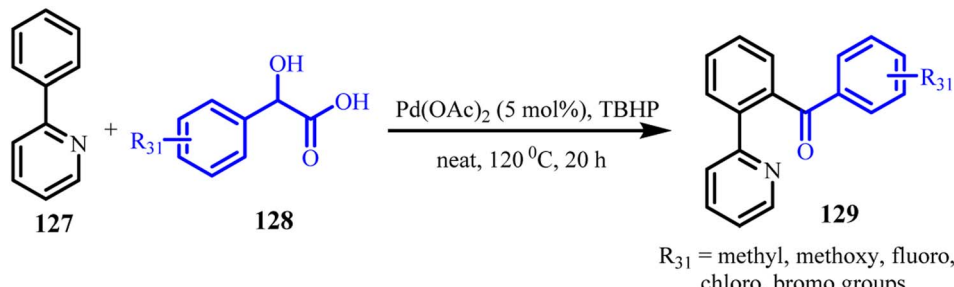
Although microbial production of vanillin through oxidative decarboxylation of vanillyl mandelic acid has been reported,<sup>114</sup> the direct microbial synthesis of ethyl vanillin (118) has been limited by the lack of suitable ethoxy-containing substrates.<sup>115</sup>

Addressing this challenge, Pan *et al.* (2013) pioneered a single-step microbial fermentation strategy for the efficient biotransformation of (S)-3-ethoxy-4-hydroxymandelic acid ((S)-EMA) (116) into ethyl vanillin (118) without generating unwanted side products. The transformation utilized a mixed resting cell system composed of two engineered recombinant strains, resulting in an efficient and eco-friendly method for ethyl vanillin production (Scheme 29).

#### 4.11. Mandelic acid derived $\alpha$ -aziridinyl alcohols as efficient ligands for asymmetric zinc organyl additions to aldehydes

The development of efficient chiral ligands for organozinc-mediated asymmetric transformations has attracted considerable attention, particularly because organozinc reagents, most notably diethylzinc, serve as versatile tools for constructing enantioenriched carbon–carbon bonds.<sup>117–119</sup> Aziridine-containing systems are especially appealing in this context, as aziridines coordinate strongly with organozinc species, thereby enhancing stereochemical control during catalytic reactions.<sup>120–122</sup> Moreover, mandelic acid derivatives offer an accessible chiral framework and can be readily incorporated

Scheme 31 Representative asymmetric transformations catalyzed by ligand 123.<sup>123</sup>



Scheme 32 Palladium-catalyzed decarboxylative cross-coupling of electron-deficient arenes with mandelic acid derivatives.<sup>124</sup>

into multifunctional ligand architectures suited for asymmetric catalysis.<sup>108</sup>

Building on these design principles, Rachwalski *et al.* (2013) introduced a family of chiral catalysts generated from (*S*)-(+)-mandelic acid (76) and an aziridine scaffold (121), producing ligands that combine secondary hydroxyl groups with  $\alpha$ -aziridinyl functionality (Scheme 30).<sup>123</sup> These structurally refined mandelic-acid-based ligands exhibited exceptional performance in the asymmetric addition of diethylzinc and phenyl-ethynylzinc to a variety of aryl and alkyl aldehydes. The resulting chiral secondary alcohols were obtained in excellent yields (up to  $\sim 95\%$ ) and with high enantioselectivities approaching 90% ee, underscoring the catalytic efficiency of these systems (Scheme 31).

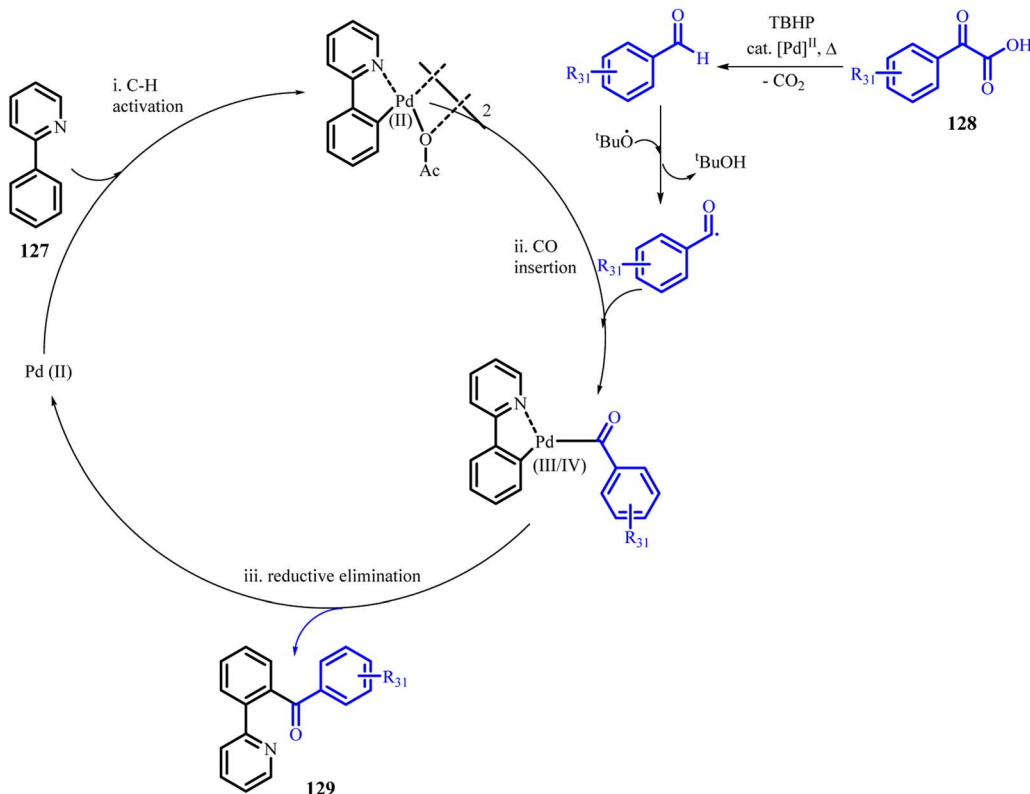
Importantly, mechanistic investigations revealed that the stereogenic center embedded within the aziridine ring exerts

a dominant influence on the stereochemical outcome of the reactions. This strong structure-reactivity correlation highlights the powerful interplay between the aziridine substituent and the mandelic-acid-derived chiral environment, ultimately enabling highly selective carbon–carbon bond formation.

Building on the role of mandelic acid derived  $\alpha$ -aziridinyl alcohols as efficient ligands in asymmetric zinc organyl additions, the discussion now advances to palladium catalyzed decarboxylative acylation of arenes using mandelic acid derivatives *via* oxidative  $sp^2$  C–H activation.

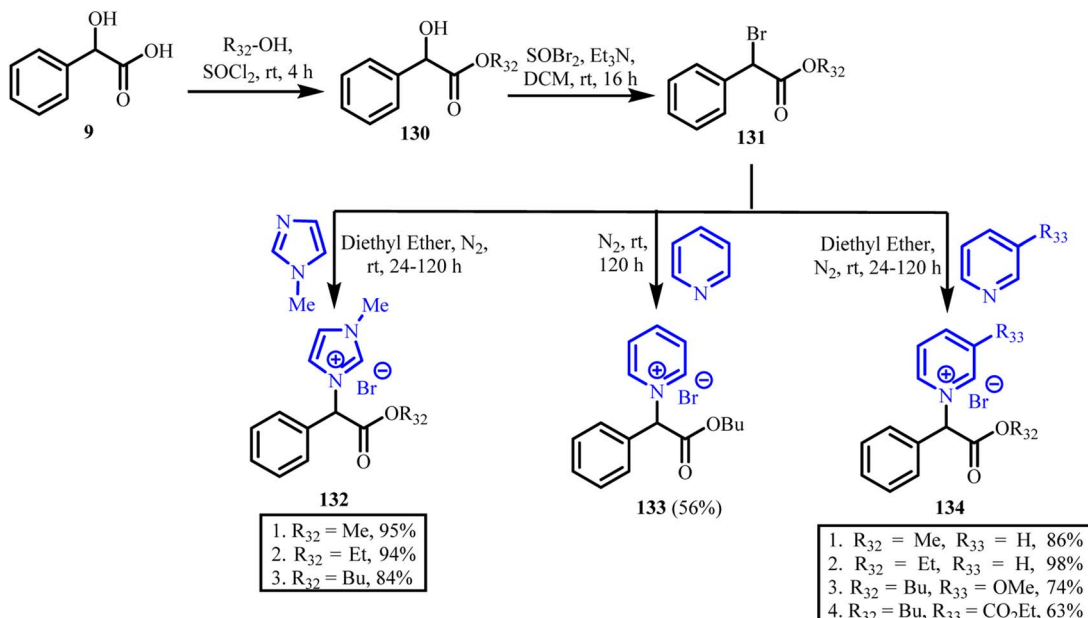
#### 4.12. Palladium-catalyzed decarboxylative acylation of arenes using mandelic acid derivatives *via* oxidative $sp^2$ C–H activation

In 2015, Liu *et al.* reported an elegant strategy for the oxidative  $sp^2$  C–H activation of arenes using *tert*-butyl hydroperoxide



Scheme 33 Proposed mechanistic route for Pd-catalyzed decarboxylative cross coupling reaction.<sup>124</sup>



Scheme 34 Synthetic route for mandelic acid-derived ester ILs.<sup>125</sup>

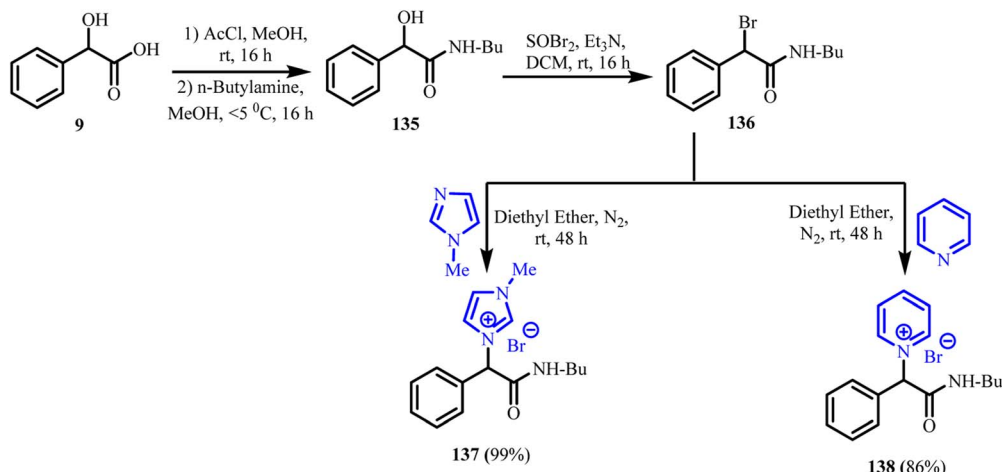
(TBHP) as the oxidant in a palladium-catalyzed acylation process, employing mandelic acid derivatives as key acyl donors (Scheme 32).<sup>124</sup> The reaction was facilitated by pyridine as an additive, which played a vital role in improving the efficiency of the catalytic system. This method offered a cost-effective, atom-economical, and environmentally benign route for the synthesis of structurally diverse aryl ketones, which are valuable intermediates in pharmaceuticals and fine chemicals. Importantly, the use of mandelic acid derivatives not only ensured ready availability but also broadened the substrate scope for the development of biologically active compounds.

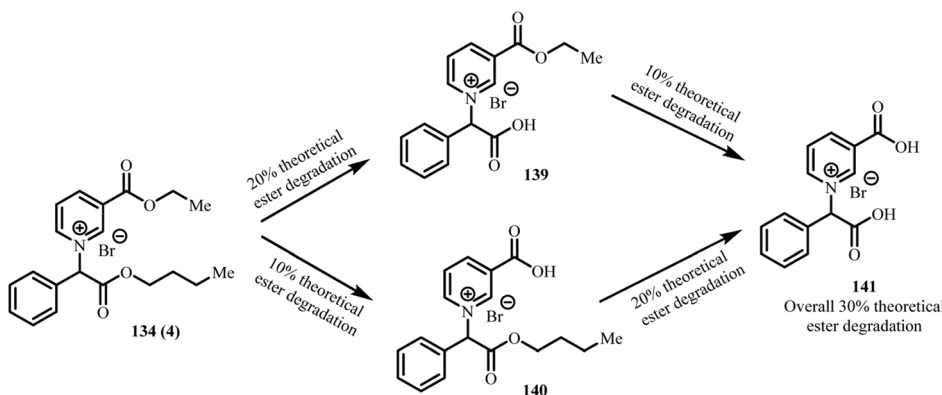
A well-considered mechanistic model was proposed, involving an initial C–H activation step, followed sequentially by carbonyl (CO) insertion and reductive elimination, ultimately leading to the formation of the desired aryl ketone product (Scheme 33).

#### 4.13. Synthesis, toxicity, and biodegradability of mandelic acid derived ionic liquids

In 2017, Prydderch *et al.* reported the synthesis of ten additional ionic liquids derived from mandelic acid derivatives, aimed at enhancing their ecological and functional profiles (Schemes 34 and 35).<sup>125</sup> Although these ILs exhibited limited antibacterial and antifungal activity, their structural modifications were strategically designed to align with the 4th, 7th, and 10th principles of green chemistry, emphasizing safer chemical design, energy efficiency, and biodegradability. The resulting ILs demonstrated improved environmental compatibility and chemical safety, underscoring their potential for greener applications in sustainable chemistry.

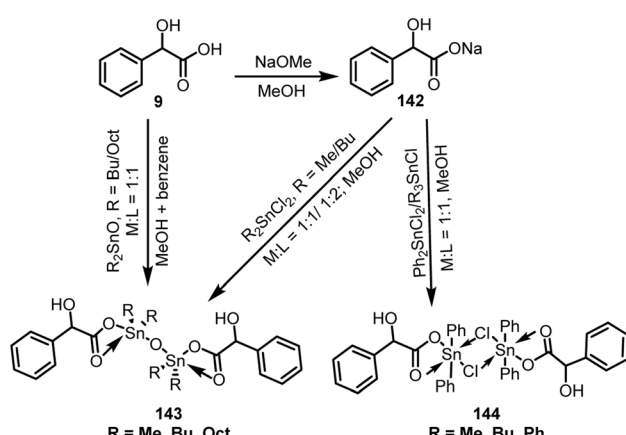
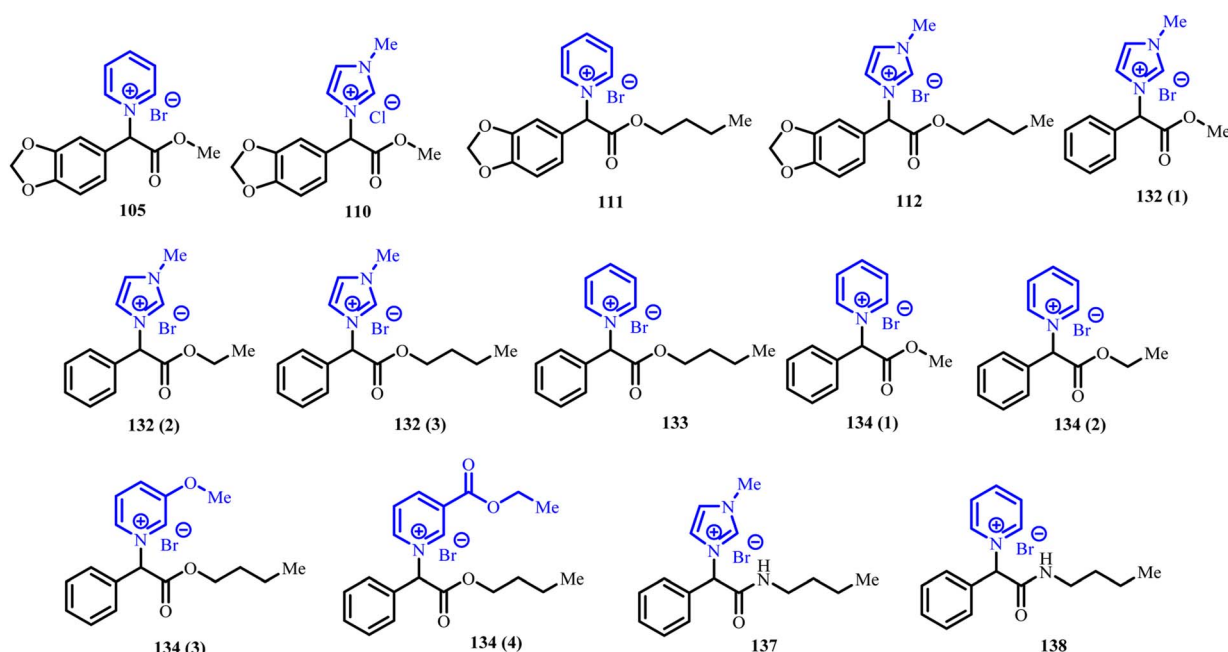
Biodegradation studies revealed that both ester- and amide-based ionic liquids (ILs) yielded the same parent carboxylic acid as the primary degradation product (Scheme 36). A

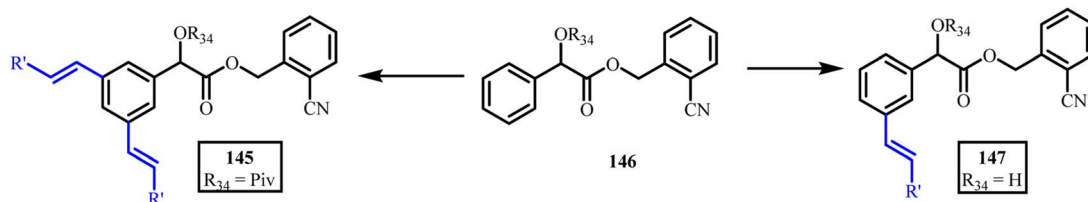
Scheme 35 Synthetic route for mandelic acid-derived amide ILs.<sup>125</sup>

Scheme 36 Proposed biodegradation pathways of ionic liquids.<sup>125</sup>

comparison between the theoretical and experimental biodegradation efficiencies, 30% for ester ILs and 31% for amide ILs, showed strong correlation, suggesting a consistent degradation pattern across both types. During the 28 days Closed Bottle Test (CBT), IL **134** (4) continued to degrade through monoester intermediates **139** and **140**, eventually converging into the major transformation product **141**. The appearance of **141** as a common final product implies that both degradation pathways likely proceed at comparable kinetic rates, highlighting a shared mechanistic route in the environmental breakdown of these ILs.

The compound set illustrated in Fig. 15 was strategically selected to encompass diverse structural features, including *n*-alkyl chains, ester or amide linkages, and *N*-heterocyclic head-groups, enabling a comprehensive assessment of their influence on ionic liquid (IL) toxicity and biodegradability.<sup>112,125</sup> Preliminary toxicity screening against twenty different bacterial and fungal strains revealed that none of the ILs exhibited notable antimicrobial activity, indicating a low ecological

Scheme 37 Synthesis of organotin(IV) mandelates as potential anti-cancer agents.<sup>138</sup>Fig. 15 Mandelic acid-derived ILs exhibiting antibacterial activity.<sup>112,125</sup>

Scheme 38 Meta-selective C-H mono- and di-olefination reactions.<sup>139</sup>

hazard profile and supporting their potential as environmentally benign alternatives in green chemistry applications.

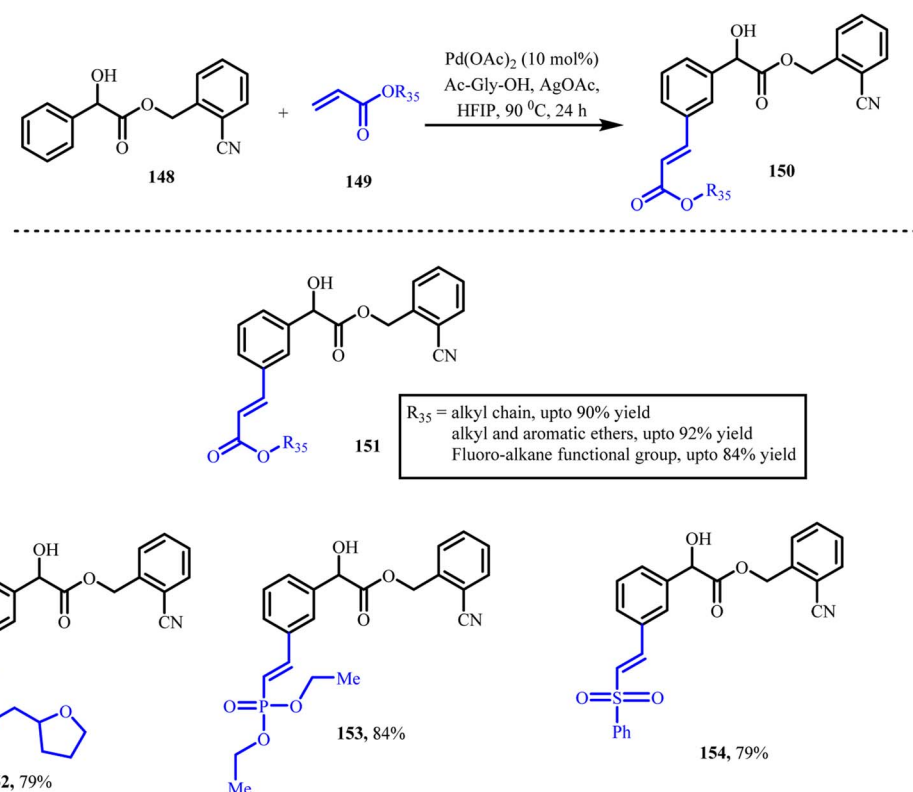
Following the exploration of the synthesis, toxicity, and biodegradability of mandelic acid-derived ionic liquids, the discussion now moves to the structure and cytotoxicity relationship of organotin(IV) mandelic acid and L-proline derivatives, highlighting their enhanced apoptotic activity.

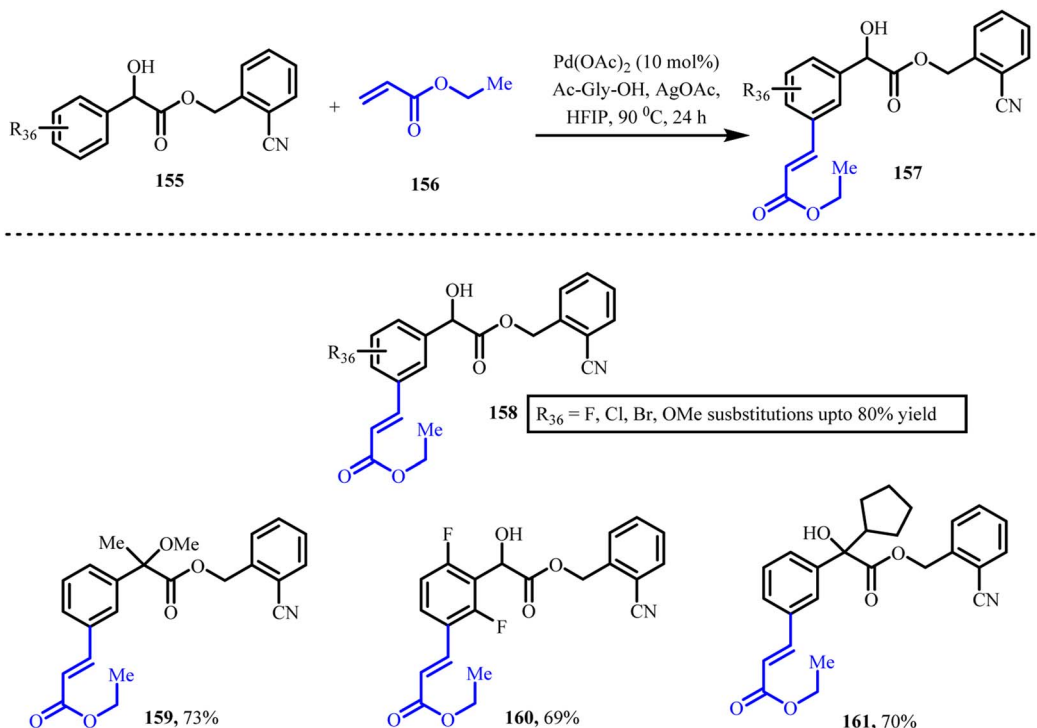
#### 4.14. Structure and cytotoxicity relationship of organotin(IV) mandelic acid and L-proline derivatives with enhanced apoptotic activity

Platinum-based anticancer agents such as *cis*-platin and *cis*-diamine dichloroplatinum(II) (CDDP) remain central to chemotherapy, yet their severe toxicity, side effects, and resistance issues continue to drive the search for alternatives.<sup>126</sup> Organotin compounds have emerged as promising candidates, with numerous studies reporting potent *in vivo* and *in vitro* anticancer activity of organotin(IV) carboxylate complexes, including activity against CDDP-resistant cell lines.<sup>127–133</sup> Among

these, dibutyltin(IV) derivatives typically display higher cytotoxicity than their methyl or phenyl analogues.<sup>134–136</sup>

Nath *et al.* previously synthesized and evaluated diorganotin(IV) mandelates, demonstrating that counter anions significantly influence biological activity.<sup>137</sup> Their subsequent 2019 study examined structure–activity relationships in mandelic acid-derived organotin(IV) complexes and compared them with related di- and tri-butyl or phenyl tin(IV) derivatives of L-proline, as well as mixed-ligand complexes incorporating 1,10-phenanthroline (Scheme 37).<sup>138</sup> These compounds showed superior anticancer potency relative to *cis*-platin and 5-fluorouracil, with low IC<sub>50</sub> values against MCF-7, HepG2, and PC-3 cell lines. Mandelic acid-based organotin(IV) complexes exhibited the highest cytotoxicity, likely due to the greater lipophilicity of the mandelate moiety, which may enhance cellular uptake. Butyl-substituted derivatives were particularly effective, outperforming their methyl and octyl analogues. Collectively, these findings position mandelic acid-derived organotin(IV) complexes as promising candidates for further development, especially against breast and prostate cancers.

Scheme 39 Meta C-H olefination of mandelic acid, adapted from ref. 139 with permission from [ACS] [Muthuraja *et al.*, 2021], copyright 2021.



**Scheme 40** Meta-selective olefination of mandelic acid derivatives, adapted from ref. 139 with permission from [ACS] [Muthuraja *et al.*, 2021], copyright 2021.

Building on the insights into the structure and cytotoxicity relationship of organotin(IV) mandelic acid and L-proline derivatives with enhanced apoptotic activity, the focus now shifts to the controlled *meta* selective C–H mono- and di-olefination of mandelic acid derivatives.

#### 4.15. Controlled *meta*-selective C–H mono- and di-olefination of mandelic acid derivatives

In 2021, Muthuraja *et al.* reported a significant advancement in the regulated *meta*-selective mono- and di-olefination of mandelic acid derivatives, as illustrated in Scheme 38.<sup>139</sup> Their study also demonstrated that the selective removal of the directing template could be achieved under mild basic conditions, leading to free *meta*-functionalized mandelic acids. The optimal conditions for *meta* C–H activation involved the use of Pd(OAc)<sub>2</sub> as the catalyst, Ac-Gly-OH as the ligand, AgOAc as the oxidant, and HFIP as the solvent. Substrate **146**, bearing a 2-cyanobenzyl directing group, afforded the *meta*-selective olefinated product with excellent regioselectivity (*meta* to *ortho* > 11 : 1), without any formation of di-olefinated by-products. Remarkably, olefins such as phenyl vinyl sulfones and vinyl phosphonate esters also furnished the desired *meta*-functionalized products with high selectivity, showcasing the broad substrate scope and efficiency of this approach.

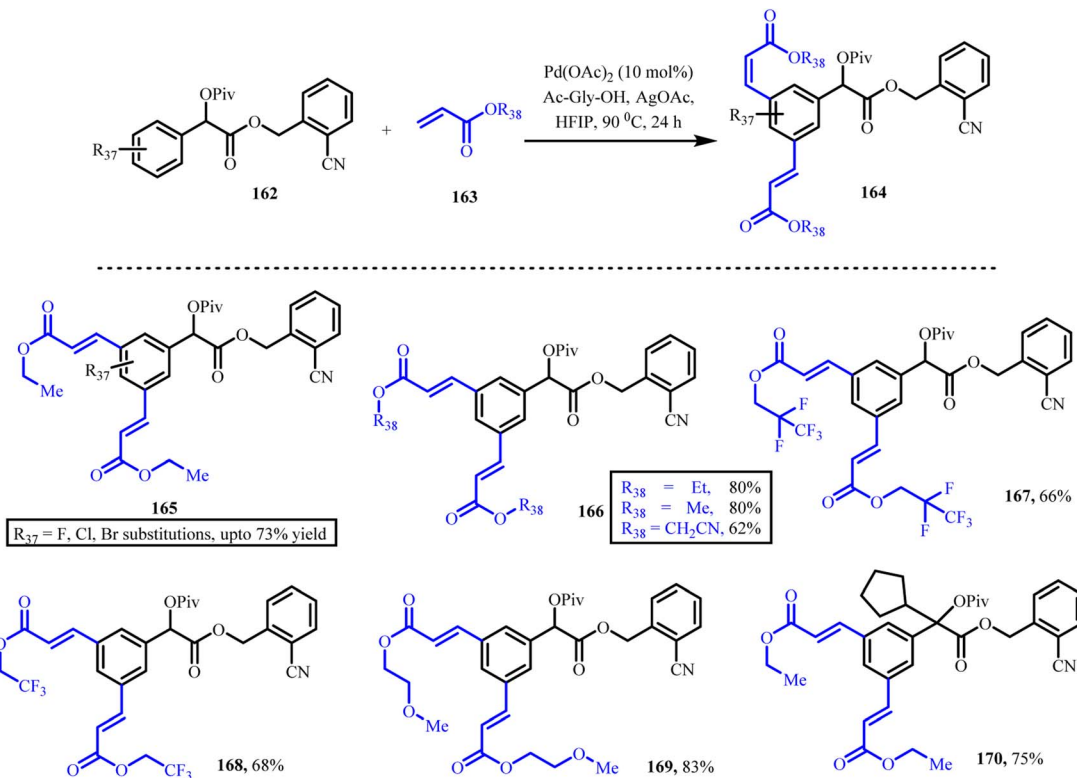
After conducting the optimized reactions on compound **148**, a highly *meta*-selective olefination was achieved with excellent yield, as shown in Scheme 39. A variety of olefin substrates were examined, among which phenyl vinyl sulfone and vinyl phosphate ester delivered the most promising outcomes.

To highlight the synthetic versatility of this strategy, a diverse range of mandelic acid derivatives was explored with

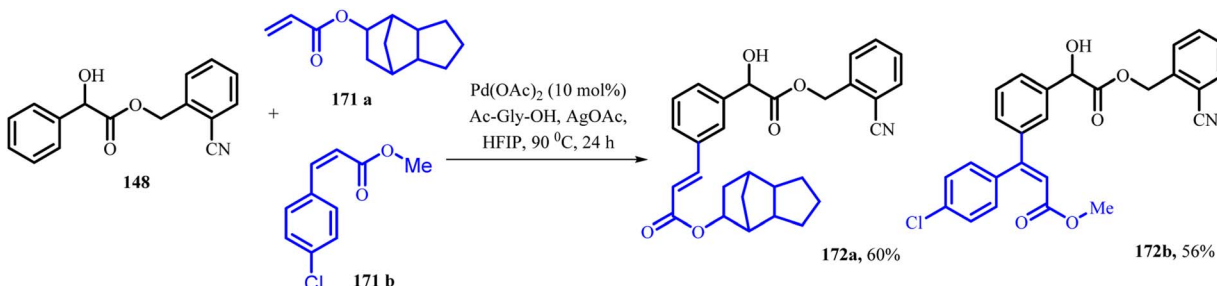
various olefin partners (Scheme 40). Most of the reactions furnished high yields along with excellent *meta*-selectivity. Substrates bearing substituents such as *p*-Cl, *p*-Br, and *p*-OMe exhibited exclusive *meta*-selectivity. In contrast, the *p*-F substituted derivative afforded a mixture of mono- and di-olefination products in a 3 : 1 ratio. Notably, substrates featuring  $\alpha$ -methyl (**159**) and cyclopentyl (**161**) groups also delivered high yields with commendable regioselectivity.

The di-olefination of mandelic acid posed a significant challenge, particularly due to selectivity issues that emerged when transitioning from mono-olefination to di-olefination. Upon further investigation, it was found that protecting the hydroxy group of mandelic acid, along with the use of silver carbonate (Ag<sub>2</sub>CO<sub>3</sub>), enabled successful di-olefination. Remarkably, even in the presence of steric hindrance along the mandelic acid side chain, the reaction proceeded with excellent *meta*-selectivity and commendable yields. A variety of acrylates, including methyl, ethyl, and methoxymethyl esters, were well tolerated, affording the corresponding di-olefinated products with high selectivity and satisfactory efficiency. Building on this success, the researchers extended the methodology to substituted mandelic acid derivatives, thereby accessing a diverse array of highly functionalized tetra-substituted benzene frameworks. This exploration highlights the broad synthetic potential and adaptability of the developed protocol (Scheme 41).

To demonstrate the practical utility of the method, sterically hindered olefins were utilized. Notably, the hindered olefin **171a** and **171b** underwent selective *meta*-olefination, affording the mono-olefinated products **172a** and **172b** in high yield, as illustrated in Scheme 42.



Scheme 41 *Meta* C–H di-olefination of protected mandelic acid, adapted from ref. 139 with permission from [ACS] [Muthuraja *et al.*, 2021], copyright 2021.



Scheme 42 *Meta* C–H olefination with sterically hindered olefin partners, adapted from ref. 139 with permission from [ACS] [Muthuraja *et al.*, 2021], copyright 2021.

Using the same strategy, the study also reported the successful synthesis of *meta*-functionalized derivatives of the drugs homatropine (175) and cyclandelate (174) (Scheme 43).

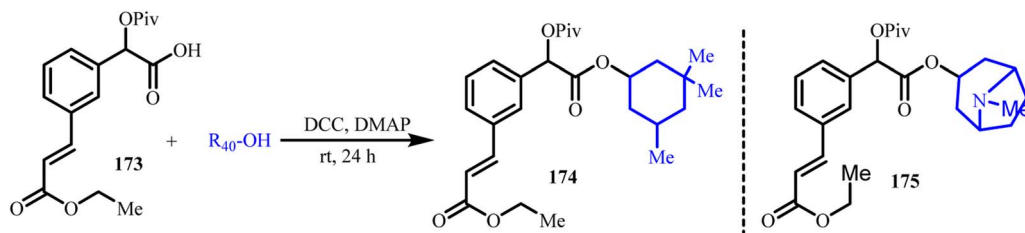
Following the discussion on controlled *meta* selective C–H mono and di-olefination of mandelic acid derivatives, attention now turns to the structure and chiral selectivity relationships of mandelic acid derivatives on modified gamma cyclodextrin gas chromatographic stationary phases.

#### 4.16. Structure and chiral selectivity relationships of mandelic acid derivatives on modified gamma-cyclodextrin gas chromatographic stationary phases

Among the many applications of mandelic acid derivatives, their use in asymmetric synthesis and chiral separation is particularly noteworthy. The combination of acidic, alcoholic, and aromatic

functionalities within a rigid framework makes mandelic acid an excellent model compound for enantioseparation.<sup>140–142</sup> Its low volatility and high polarity also favour derivatization for gas chromatography (GC). Cyclodextrins are widely used in GC and capillary electrophoresis because their hydrophobic cavities can encapsulate suitable analytes,<sup>143,144</sup> and 6-*tert*-butyldimethylsilyl cyclodextrin derivatives display broad chiral selectivity in GC, enabling efficient separation of diverse enantiomers.<sup>145–148</sup> Nevertheless, chiral resolution often remains empirical and system-dependent.

Repassy *et al.* (2023) evaluated a chiral selector composed of octakis 2,3-di-*O*-acetyl-6-*O*-*tert*-butyldimethylsilyl gamma-cyclodextrin (TBDMSDAGCD) mixed with a silicon polymer stationary phase.<sup>149</sup> This host–guest system enables electron donor–acceptor and hydrogen-bonding interactions. Mandelic acid and 20 of its substituted derivatives (Fig. 16) were



**Scheme 43** Synthesis of cyclandelate (174) and homatropine derivative (175), adapted from ref. 139 with permission from [ACS] [Muthuraja *et al.*, 2021], copyright 2021.

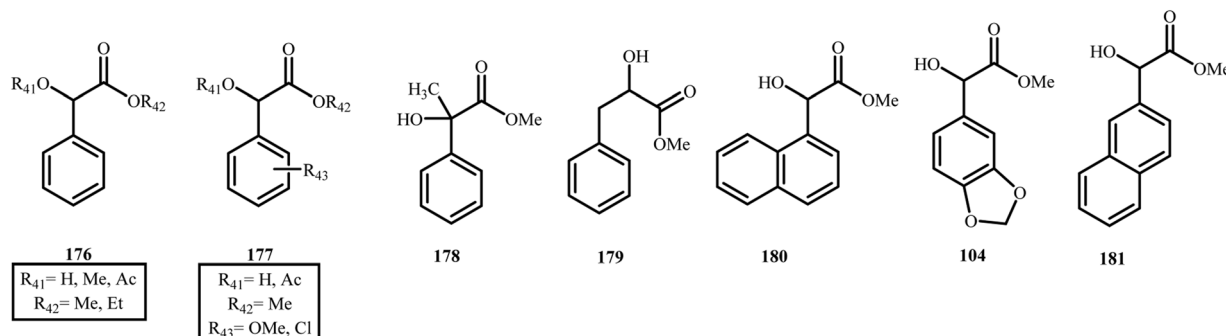


**Fig. 16** Mandelic acid derivatives as model compounds to test the chiral selectivity of TBDMSDAGCD.<sup>149</sup>

examined to assess chiral recognition. Compounds containing hydrogen-bond donor groups (free carboxyl or hydroxyl functions) showed excellent selectivity, attributed to the strong hydrogen-bond acceptor properties of TBDMSDAGCD. Even derivatives lacking these donors (*e.g.*, methyl ethers, acetates) exhibited measurable but lower enantioseparation.

For aromatic ring-substituted derivatives, chiral selectivity depended largely on the extent of inclusion in the cyclodextrin cavity, with *para*-substituted compounds displaying the highest selectivity. Notably, enantiomer elution order reversed when comparing derivatives with free hydroxyl groups to their acetate-protected analogues.

Overall, these results establish TBDMSDAGCD as a highly effective and broadly compatible chiral selector for resolving mandelic acid derivatives.

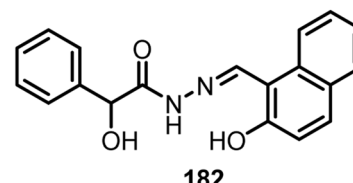
#### 4.17. Synthesis, structural characterization, and catalytic efficiency of metal chelates of mandelic acid hydrazone derivatives

Hydrazone-based ligands, known for their excellent coordination capabilities, have emerged as versatile systems in both organic and inorganic chemistry.<sup>150,151</sup> Due to their multiple bonding modes with various metal centres, hydrazone compounds and their metal chelates have shown broad applicability across several domains, ranging from biological activities such as antimicrobial and antibiotic effects to roles in molecular sensing, luminescent probes, catalysis, and analytical applications.<sup>152-159</sup> Among transition metals, manganese plays a significant role in biological processes, including metabolism, antioxidant defence mechanisms, and oxygen

evolution in photosynthesis.<sup>159-161</sup> In addition, manganese-coordinated compounds have attracted considerable interest for their catalytic activity, especially when coordinated with Schiff base ligands containing nitrogen and oxygen donor atoms.<sup>162</sup>

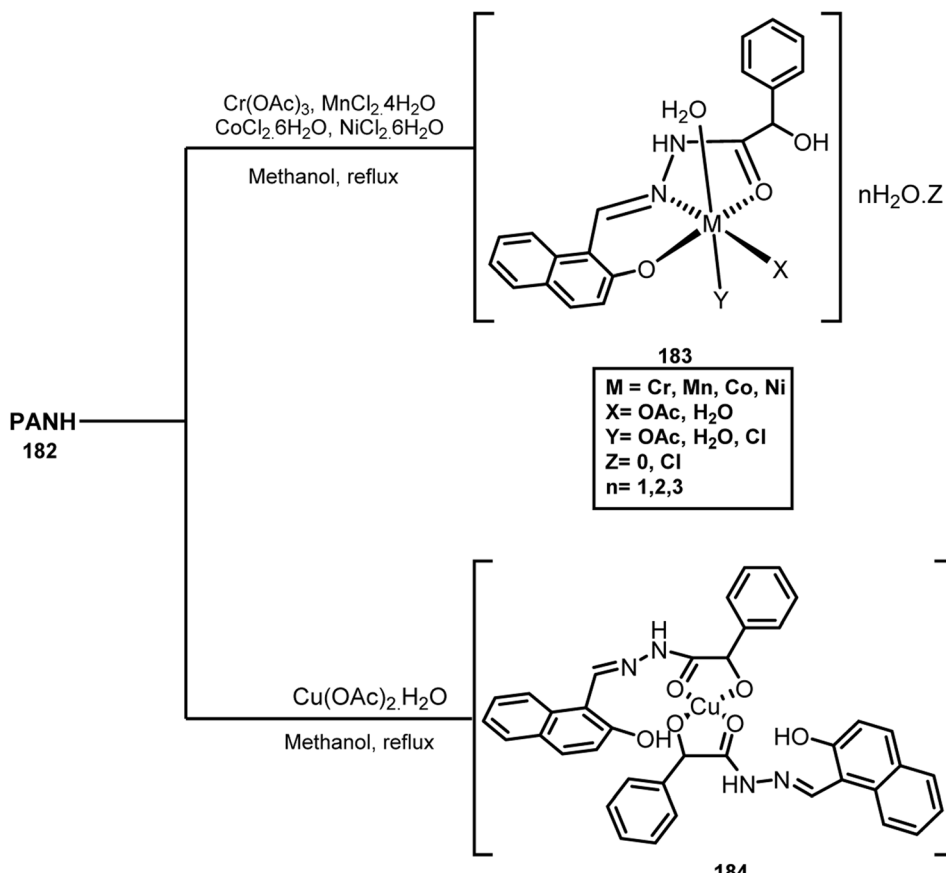
Manganese complexes have become particularly important in the development of biomimetic catalysts for oxidase-like functions, such as catecholase, phenoxazinone synthase, and oxygenase. In pharmaceutical applications, the phenoxazinone chromophore, which inhibits transcription (DNA to RNA conversion) in tumor cells, is used to treat Wilms' tumor.<sup>163</sup> Other metal complexes, including those of copper(II), cobalt(II), and ruthenium(II), have also demonstrated effective phenoxazinone synthase activity, provided they offer sufficient lability at the metal coordination sites.<sup>163-165</sup>

In 2024, El-Ghamri *et al.* reported the synthesis of a novel Schiff base ligand derived from mandelic acid hydrazone, namely hydroxy-phenyl-acetic acid (2-hydroxy-naphthalen-1-ylmethylene) hydrazide (PANH) (182) (Fig. 17). This ligand was employed to coordinate with chromium(III), manganese(II), cobalt(II), nickel(II), and copper(II) ions for the development of



**Fig. 17** Structure of hydroxy-phenyl-acetic acid (2-hydroxynaphthalen-1-ylmethylene)hydrazide (PANH).<sup>166</sup>



Scheme 44 PANH-metal complexes.<sup>166</sup>

catalysts mimicking phenoxazinone synthase activity (**183**, **184**).<sup>166</sup> Comprehensive spectroscopic analyses were conducted to determine the geometry, bonding interactions, electrolytic nature, and magnetic properties of the complexes.

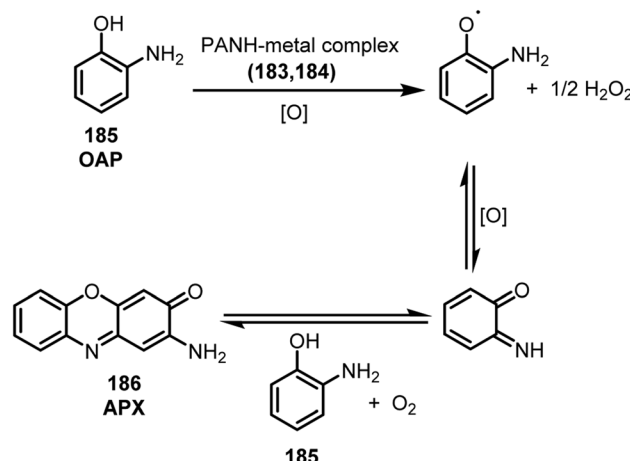
To evaluate their catalytic efficiency, the PANH-metal complexes (Scheme 44) were tested for the oxidation of *o*-aminophenol (OAP) (**185**) to 2-aminophenoxazine-3-one (APX) (**186**) (Scheme 45), the target transformation catalyzed by phenoxazinone synthase. The manganese(II) complex exhibited outstanding catalytic activity, achieving a turnover frequency (TOF) of 169.89 h<sup>-1</sup>. Other complexes demonstrated comparatively lower efficiencies, following the order PANH-Co > PANH-Cu > PANH-Ni, with TOF values ranging from 0.048 to 0.0948 h<sup>-1</sup>. Interestingly, the chromium(III) complex showed no catalytic activity.

Further investigation revealed that the catalytic performance was influenced not only by the metal center but also by the type of counter anion. All catalytically active complexes contained chloride ions, while the inactive chromium complex featured acetate as the counter anion. The reduced activity in the latter case was attributed to the steric hindrance imposed by the bulkier acetate group, which restricted access to the labile coordination sites in the first coordination sphere. In contrast, the smaller chloride ion allowed for more accessible coordination sites, facilitating substrate interaction. Thus, both the oxidation state of the metal and the nature of the counter anion

were found to be critical factors in determining the catalytic efficiency of these PANH-based metal complexes (**183**, **184**).

#### 4.18. Discussion: chemical innovations and functional insights of mandelic acid derivatives

$\alpha$ - and  $\beta$ -hydroxy carboxylic acids are widely distributed in nature, where they appear in numerous microorganisms and

Scheme 45 Oxidation of *o*-aminophenol (OAP) to 2-aminophenoxazine-3-one (APX) catalyzed by PANH-metal complexes.<sup>166</sup>

serve as key intermediates in both  $\alpha$ - and  $\beta$ -oxidation pathways during fatty-acid metabolism.<sup>167,168</sup> Beyond their biological relevance,  $\alpha$ -hydroxy acids occupy an important position in synthetic chemistry. They are frequently employed as chiral building blocks, serve as versatile chiral ligands in asymmetric catalysis, and are routinely used as resolving agents for a variety of alcohols and amines. Their utility even extends to industrial formulations, including their incorporation as anti-aging constituents in cosmetic products. Owing to this broad spectrum of applications, ranging from biochemical processes to synthetic and industrial uses, the pursuit of efficient and innovative synthetic strategies for accessing these valuable molecules continues to be an active and widely explored area of research. Given the importance of  $\alpha$ -hydroxy acids within both natural and synthetic contexts, particular attention has been directed toward mandelic acid, a representative  $\alpha$ -hydroxy acid with exceptional structural and functional attributes.<sup>167,169</sup>

Mandelic acid stands out as a remarkable chiral scaffold, prized for its ready availability, inherent stereochemistry, and versatile functional groups. This combination has spurred its extensive application across asymmetric synthesis, catalysis, and materials science, making it a cornerstone in modern chemical research.

Early explorations leveraged mandelic acid to craft  $\alpha$ -hydroxy-2-oxazolines, chiral ligands that enable asymmetric phenyl transfer to aromatic aldehydes. The work of Bolm and co-workers revealed that such ligands, derived through condensation and cyclization steps, could deliver moderate but promising enantioselectivity, establishing mandelic acid's potential in asymmetric transformations. Building on this foundation, subsequent studies demonstrated highly diastereoselective arylations using the (*S*)-mandelic acid enolate, efficiently producing enantiomerically pure oxindoles, benzylic acids, and nitrobenzophenones. These advances cleverly harnessed aerobic oxidative decarboxylation catalyzed by cobalt complexes, underscoring mandelic acid's adaptability and the subtle interplay between redox mediators and reaction pathways, exemplified by the multifaceted role of nitrobenzene.

The versatility of mandelic acid enolates extends further into stereoselective Michael additions with  $\alpha,\beta$ -enones, furnishing key 2-substituted 1,4-diketones building blocks for bioactive molecules such as jasmones and prostaglandins. Intriguingly, the stereochemical outcome depends critically on lithium coordination and the presence of additives like HMPA. This additive disrupts chelated transition states, shifting the reaction mechanism to less stereoselective pathways. Such findings elegantly highlight how metal ion coordination and subtle changes in the reaction environment dramatically steer enantioselectivity and diastereocontrol.

The utility of mandelic acid derivatives also shines in the enantioselective synthesis of non-symmetrical benzoin. Mechanistic insights rooted in Seebach's principles revealed how facial selectivity arises from kinetically favoured transition states, enabling predictable and high-fidelity stereochemical outcomes. This elegant stereochemical control is a testament to the power of mandelic acid scaffolds in orchestrating complex molecular architectures with precision.

Beyond chemical synthesis, mandelic acid derivatives have found synergy with biotechnological approaches. Recombinant *Escherichia coli* strains have been engineered to catalyze selective oxidative decarboxylation, facilitating green, single-step production of ethyl vanillin—a flavour compound prized for its stability and aroma. This biocatalytic strategy not only mitigates environmental concerns inherent to traditional chemical routes but also showcases mandelic acid's compatibility with sustainable manufacturing.

In parallel, the synthesis of imidazolium and pyridinium ionic liquids (ILs) from mandelic acid derivatives has generated promising "green" solvents characterized by low toxicity and high biodegradability. Detailed toxicity assessments and degradation studies confirmed these ILs' environmental safety, aligning them with modern principles of sustainable chemistry. The design of such ILs balances physicochemical performance with ecological responsibility, positioning mandelic acid as a valuable platform for future solvent innovation.

Mandelic acid's influence extends into organometallic catalysis, where  $\alpha$ -aziridinyl alcohol derivatives serve as efficient chiral ligands in zinc-mediated additions to aldehydes, delivering chiral secondary alcohols in high yield and enantiopurity. The stereogenic centres on these ligands orchestrate reactivity with remarkable selectivity, further enriching asymmetric synthesis toolkits.

Palladium-catalyzed decarboxylative acylation reactions elegantly employ mandelic acid derivatives as acyl donors in oxidative  $sp^2$  C–H activation of arenes. This atom-economical, cost-effective approach broadens access to diverse aryl ketones, key intermediates in pharmaceuticals and fine chemicals, while embodying environmentally benign methodology.

Continued exploration of mandelic acid-derived ILs has fine-tuned their chemical safety profiles, emphasizing biodegradability and minimal antimicrobial activity to mitigate ecological hazards. Complementary research on organotin(IV) mandelic acid and L-proline complexes reveals their potent anticancer activity, often surpassing that of conventional platinum drugs. The structure–activity relationships elucidated indicate that both lipophilicity and ligand identity crucially influence cellular uptake and cytotoxicity, heralding these complexes as promising therapeutic candidates.

The synthetic versatility of mandelic acid is further exemplified by advancements in controlled *meta*-selective C–H olefination. This Pd-catalyzed methodology enables precise mono- and di-olefination even in sterically challenging substrates, yielding highly functionalized aromatic frameworks. Its applicability to pharmaceutical derivatives like homatropine and cyclandelate highlights real-world utility, while the method's broad substrate scope and high regioselectivity underscore its synthetic power.

Mandelic acid also excels in chiral separation technologies. Modified gamma-cyclodextrin stationary phases capitalize on mandelic acid derivatives' acidic and hydroxyl functionalities to achieve remarkable enantioselectivity in gas chromatography. Hydrogen bonding and host–guest inclusion interactions govern this chiral recognition, providing insightful guidance for empirical optimization of resolution protocols.

Finally, metal chelates of mandelic acid hydrazone derivatives mimic biologically important enzymes such as



phenoxazinone synthase. Among these, manganese(II) complexes stand out for their exceptional catalytic turnover, with the nature of counter anions playing a pivotal role in modulating activity by controlling access to coordination sites. These studies offer valuable blueprints for designing biomimetic catalysts with tunable performance.

In essence, mandelic acid derivatives weave a rich tapestry across synthetic methodology, catalysis, biotechnology, green chemistry, and biomedical applications. The nuanced understanding of reaction mechanisms, coordination chemistry, and environmental interactions continues to unlock their full potential, promising new frontiers in both fundamental research and practical innovation.

## 5 Conclusion and future perspectives

Mandelic acid and its diverse derivatives have firmly established themselves as a remarkably versatile class of compounds, bridging the realms of chemistry and biology with impressive breadth and depth. As this review has illuminated, these  $\alpha$ -hydroxy aromatic acids serve not only as privileged pharmacophores in medicinal chemistry, demonstrating potent activities ranging from  $\pi$  inhibition and antiviral effects to antimicrobial, anti-inflammatory, and enzyme inhibitory properties—but also as promising agents in plant protection and beyond. Their multifunctional nature is further amplified through scaffold hybridization, which has propelled the design of novel derivatives featuring phthalimides, pyrazoles, and oxadiazoles, enhancing biological selectivity and pharmacokinetic profiles.

On the chemical front, the synthetic adaptability of mandelic acid derivatives has enabled their transformation into functional biomaterials and green solvents, heralding innovative applications in drug delivery and sustainable chemistry. Cutting-edge methodologies—such as stereoselective enolate additions, palladium-catalyzed C–H activations, and biocatalytic oxidative transformations—underscore the dynamic landscape of synthetic advances harnessing mandelic acid's intrinsic chirality and reactivity.

Looking ahead, the future of mandelic acid derivatives is ripe with exciting opportunities and challenges. Deepening our understanding of structure–activity relationships (SAR) through integrative computational and experimental approaches will be pivotal for designing derivatives with pinpoint biological specificity and reduced off-target effects. The integration of green and scalable synthetic methods is imperative to bridge laboratory innovation with industrial viability, ensuring sustainable production aligned with environmental imperatives.

Emerging paradigms such as multitarget-directed ligands (MTDLs) offer tantalizing prospects for leveraging mandelic acid scaffolds to simultaneously modulate complex disease pathways, a promising avenue especially for multifactorial diseases like cancer and neurodegenerative disorders. The convergence of nanotechnology and responsive delivery platforms opens transformative possibilities for precision-targeted therapeutics, enhancing efficacy while minimizing systemic side effects.

Moreover, mandelic acid derivatives' untapped potential in agriculture invites intensified exploration toward developing

eco-friendly agrochemicals that could revolutionize sustainable plant disease management. Crucially, moving beyond *in vitro* assays, rigorous *in vivo* evaluations and comprehensive clinical studies are indispensable to translate the compelling bioactivities of these compounds into safe and effective therapies.

In essence, mandelic acid derivatives epitomize a dynamic intersection of chemical ingenuity and biological relevance. Their journey from bench to bedside—and potentially from field to fork—will be driven by interdisciplinary collaborations that meld synthetic chemistry, pharmacology, materials science, and agriscience. As research continues to unravel their multifaceted capabilities, mandelic acid derivatives are poised to inspire innovative solutions that address pressing challenges in health, environment, and beyond.

## Author contributions

AB initially prepared the draft following the suggestions of AKM. AKM later modified and rewrote the manuscript according to the standard of the journal.

## Conflicts of interest

The authors declare that there is no conflict of interest.

## Data availability

No new data were created or analyzed in this study. Data sharing is not applicable to this article.

## Acknowledgements

Amit Banerjee would like to acknowledge his parents for their support and encouragement during this work. This research did not receive any specific grant from funding agencies in the public, commercial, or not-for-profit sectors.

## References

- 1 (a) F. L. Winckler, *Repertorium für die Pharmacie*, 1831, vol. 38, pp. 169–196; (b) F. L. Winckler, *Ann. Chem. Pharm.*, 1832, **18**, 310–319.
- 2 L. Martínková and V. Křen, *Appl. Microbiol. Biotechnol.*, 2018, **102**, 3893–3900.
- 3 Y.-C. He, J.-H. Xu, J. Pan, L.-M. Ouyang and Y. Xu, *Bioprocess Biosyst. Eng.*, 2007, **31**, 445–451.
- 4 H. G. Brittain, *Analytical Profiles of Drug Substances and Excipients*, Academic Press, 2002, 179–211.
- 5 R. V. Singh and K. Sambyal, *Crit. Rev. Biotechnol.*, 2022, **43**, 1226–1235.
- 6 R. Choińska, K. Dąbrowska, R. Świsłocka, W. Lewandowski and A. H. Świergiel, *Mini-Rev. Med. Chem.*, 2021, **21**, 2544–2550.
- 7 R. M. Dębowska, A. Kaszuba, I. Michalak, A. Dzwigałowska, C. Cieścińska, E. Jakimiuk, J. Zielińska and A. Kaszuba, *Dermatol. Rev.*, 2015, **4**, 316–321.

8 S. Jacobs and E. Culbertson, *Facial Plast. Surg.*, 2018, **34**, 651–656.

9 J. K. Whitesell and D. Reynolds, *J. Org. Chem.*, 1983, **48**, 3548–3551.

10 Q. Wang, S. Geng, L. Wang, Z. Wen, X. Sun and H. Huang, *J. Appl. Microbiol.*, 2022, **133**, 273–286.

11 J. Yin, Y. An and H. Gao, *Microorganisms*, 2025, **13**, 1722.

12 S. R. M. Ibrahim, A. Sirwi, B. G. Eid, S. G. A. Mohamed and G. A. Mohamed, *Metabolites*, 2021, **11**, 683.

13 W. Sun and M. H. Shahrazabian, *Molecules*, 2023, **28**, 1845.

14 Y. Li, J. Sun, Z. Fu, Y. He, X. Chen, S. Wang, L. Zhang, J. Jian, W. Yang, C. Liu, X. Liu, Y. Yang and Z. Bai, *Biotechnol. Biofuels Bioprod.*, 2024, **17**, 130.

15 S. Naz, M. Zahoor, M. N. Umar, S. Alghamdi, M. U. K. Sahibzada and W. UlBari, *Open Chem.*, 2020, **18**, 764–777.

16 B. Heasley, *Curr. Org. Chem.*, 2014, **18**, 641–686.

17 M. Jung, S. Lee, H. Kim and H. Kim, *Curr. Med. Chem.*, 2000, **7**, 649–661.

18 T. Goel, N. Jain and D. Bansode, *Lett. Org. Chem.*, 2023, **21**, 320–332.

19 C. A. Fewson, *FEMS Microbiol. Lett.*, 1988, **54**, 85–110.

20 H. Brandstetter, A. Kühne, W. Bode, R. Huber, W. Von Der Saal, K. Wirthensohn and R. A. Engh, *J. Biol. Chem.*, 1996, **271**, 29988–29992.

21 B.-Y. Zhu and R. M. Scarborough, *Annu. Rep. Med. Chem.*, 2000, 83–102.

22 J. M. Fevig and R. R. Wexler, *Annu. Rep. Med. Chem.*, 1999, 81–100.

23 R. M. Scarborough, *J. Enzyme Inhib. Med. Chem.*, 1998, **14**, 15–25.

24 G. Claeson, *Blood Coagul. Fibrinolysis*, 1994, **5**(3), 411–436.

25 T. Su, Y. Wu, B. Doughan, K. Kane-Maguire, C. K. Marlowe, J. P. Kanter, J. Woolfrey, B. Huang, P. Wong, U. Sinha, G. Park, J. Malinowski, S. Hollenbach, R. M. Scarborough and B.-Y. Zhu, *Bioorg. Med. Chem. Lett.*, 2001, **11**, 2279–2282.

26 L. J. D. Zaneveld, *US Pat.* 6028115, 2000.

27 J. K. Whitesell and J. A. Pojman, *Chem. Mater.*, 1990, **2**, 248–254.

28 H. Fukuzaki, Y. Aiba, M. Yoshida, M. Asano and M. Kumakura, *Macromol. Chem. Phys.*, 1989, **190**, 2407–2415.

29 M. Ward, B. Yu, V. Wyatt, J. Griffith, T. Craft, A. R. Neurath, N. Strick, Y.-Y. Li, D. L. Wertz, J. A. Pojman and A. B. Lowe, *Biomacromolecules*, 2007, **8**, 3308–3316.

30 N. Kushwaha and D. Kaushik, *J. Appl. Pharm. Sci.*, 2016, 159–171.

31 N. M. Jamel, K. A. Al-Hammed and B. j Ahmed, *J. Pharm. Sci. Res.*, 2019, **11**, 3348–3354.

32 L. M. Lima, P. Castro, A. L. Machado, C. A. M. Fraga, C. Lugnier, V. L. G. De Moraes and E. J. Barreiro, *Bioorg. Med. Chem.*, 2002, **10**, 3067–3073.

33 R. Varala, V. Kotra, M. M. Alam, N. R. Kumar, S. Ganapaty and S. R. Adapa, *Indian J. Chem., Sect. B: Org. Chem. Incl. Med. Chem.*, 2008, **47**, 1243–1248.

34 C. D. Stan, A. Ştefanache, G. Tătărîngă, M. Drăgan and C. G. Tuchiluş, *Farmacia*, 2015, **63**, 577–580.

35 S. Savary, P. S. Teng, L. Willocquet and F. W. Nutter, *Annu. Rev. Phytopathol.*, 2006, **44**, 89–112.

36 N. Concha, J. Huang, X. Bai, A. Benowitz, P. Brady, L. C. Grady, L. H. Kryn, D. Holmes, K. Ingraham, Q. Jin, L. P. Kaushansky, L. McCloskey, J. A. Messer, H. O'Keefe, A. Patel, A. L. Satz, R. H. Sinnamon, J. Schneck, S. R. Skinner, J. Summerfield, A. Taylor, J. D. Taylor, G. Evindar and R. A. Stavenger, *J. Med. Chem.*, 2016, **59**, 7299–7304.

37 S. Fustero, R. Román, J. F. Sanz-Cervera, A. Simón-Fuentes, J. Bueno and S. Villanova, *J. Org. Chem.*, 2008, **73**, 8545–8552.

38 D.-Y. Hu, Q.-Q. Wan, S. Yang, B.-A. Song, P. S. Bhadury, L.-H. Jin, K. Yan, F. Liu, Z. Chen and W. Xue, *J. Agric. Food Chem.*, 2008, **56**, 998–1001.

39 Y. Ali, M. S. Alam, H. Hamid, A. Husain, A. Dhulap, S. Bano, C. Kharbanda, S. Nazreen and S. Haider, *Med. Chem. Res.*, 2015, **24**, 3775–3784.

40 N. Nayak, J. Ramprasad, U. Dalimba, P. Yogeeswari, D. Sriram, H. S. S. Kumar, S. K. Peethambar and R. Achur, *Res. Chem. Intermed.*, 2015, **42**, 3721–3741.

41 N. F. El-Sayed, E. F. Ewies, M. El-Hussieny, L. S. Boulos and E. M. Shalaby, *Z. Naturforsch. B*, 2016, **71**, 765–776.

42 Y. Xie, X. Ruan, H. Gong, Y. Wang, X. Wang, J. Zhang, Q. Li and W. Xue, *J. Heterocycl. Chem.*, 2017, **54**, 2644–2649.

43 C. T. Supuran, *Nat. Rev. Drug Discovery*, 2008, **7**, 168–181.

44 E. Švastová, A. HuliKová, M. Rafajová, M. Zat'ovičová, A. Gibadulinová, A. Casini, A. Cecchi, A. Scozzafava, C. T. Supuran, J. Pastorek and S. Pastoreková, *FEBS Lett.*, 2004, **577**, 439–445.

45 M. Hilvo, L. Baranauskiene, A. M. Salzano, A. Scaloni, D. Matulis, A. Innocenti, A. Scozzafava, S. M. Monti, A. Di Fiore, G. De Simone, M. Lindfors, J. Jänis, J. Valjakka, S. Pastoreková, J. Pastorek, M. S. Kulomaa, H. R. Nordlund, C. T. Supuran and S. Parkkila, *J. Biol. Chem.*, 2008, **283**, 27799–27809.

46 S. M. Monti, C. T. Supuran and G. De Simone, *Curr. Med. Chem.*, 2012, **19**, 821–830.

47 A. Akdemir, Ö. Güzel-Akdemir, A. Scozzafava, C. Capasso and C. T. Supuran, *Bioorg. Med. Chem.*, 2013, **21**, 5228–5232.

48 S. Carradori, A. Mollica, M. Ceruso, M. D'Ascenzio, C. De Monte, P. Chimenti, R. Sabia, A. Akdemir and C. T. Supuran, *Bioorg. Med. Chem.*, 2015, **23**, 2975–2981.

49 M. D'Ascenzio, P. Guglielmi, S. Carradori, D. Secci, R. Florio, A. Mollica, M. Ceruso, A. Akdemir, A. P. Sobolev and C. T. Supuran, *J. Enzyme Inhib. Med. Chem.*, 2016, **32**, 51–59.

50 Ö. Güzel-Akdemir, A. Akdemir, N. Karali and C. T. Supuran, *Org. Biomol. Chem.*, 2015, **13**, 6493–6499.

51 C. T. Supuran, *J. Enzyme Inhib. Med. Chem.*, 2015, **31**, 345–360.

52 Ö. Güzel-Akdemir, A. Angeli, K. Demir, C. T. Supuran and A. Akdemir, *J. Enzyme Inhib. Med. Chem.*, 2018, **33**, 1299–1308.



53 S. Hou, D. Xie, J. Yang, X. Niu, D. Hu and Z. Wu, *Chem. Biol. Drug Des.*, 2021, **98**, 166–174.

54 S. Hou, H. Shi, H. Zhang, Z. Wu and D. Hu, *J. Agric. Food Chem.*, 2023, **71**, 7631–7641.

55 H. Shi, L. Li, D. Song, Y. Zheng and Z. Wu, *Arabian J. Chem.*, 2023, **16**, 104884.

56 B. Chen, D. Song, H. Shi, K. Chen, Z. Wu and H. Chai, *Int. J. Mol. Sci.*, 2023, **24**, 8898.

57 Q. Guo, Y. Li, H. Shi, A. Yi, X. Xu, H. Wang, X. Deng, Z. Wu and Z. Cui, *Pest Manage. Sci.*, 2023, **79**, 4626–4634.

58 L. A. Rigano, M. R. Marano, A. P. Castagnaro, A. M. D. Amaral and A. A. Vojnov, *BMC Microbiol.*, 2010, **10**, 176.

59 E. Shahbaz, M. Ali, M. Shafiq, M. Atiq, M. Hussain, R. M. Balal, A. Sarkhosh, F. Alferez, S. Sadiq and M. A. Shahid, *Plants*, 2022, **12**, 123.

60 D. A. Rasko and V. Sperandio, *Nat. Rev. Drug Discovery*, 2010, **9**, 117–128.

61 G. R. Cornelis, *Nat. Rev. Microbiol.*, 2006, **4**, 811–825.

62 D. Büttner, *Microbiol. Mol. Biol. Rev.*, 2012, **76**, 262–310.

63 N. C. Marshall and B. B. Finlay, *Expert Opin. Ther. Targets*, 2013, **18**, 137–152.

64 A. Yamazaki, J. Li, Q. Zeng, D. Khokhani, W. C. Hutchins, A. C. Yost, E. Biddle, E. J. Toone, X. Chen and C.-H. Yang, *Antimicrob. Agents Chemother.*, 2011, **56**, 36–43.

65 L.-L. He, X. Wang, D. O. Rothenberg, X. Xu, H.-H. Wang, X. Deng and Z.-N. Cui, *Pestic. Biochem. Physiol.*, 2023, **194**, 105471.

66 L. K. Tsou, M. Lara-Tejero, J. RoseFigura, Z. J. Zhang, Y.-C. Wang, J. S. Yount, M. Lefebvre, P. D. Dossa, J. Kato, F. Guan, W. Lam, Y.-C. Cheng, J. E. Galán and H. C. Hang, *J. Am. Chem. Soc.*, 2016, **138**, 2209–2218.

67 H. Tao, H. Tian, S. Jiang, X. Xiang, Y. Lin, W. Ahmed, R. Tang and Z.-N. Cui, *Pestic. Biochem. Physiol.*, 2019, **160**, 87–94.

68 D. Gao, H. Li, J. Shao, L. He, C. Fu, H. Lai, D. O. Rothenberg, X. Xu, G. Song, X. Deng and Z.-N. Cui, *J. Agric. Food Chem.*, 2023, **71**, 9291–9301.

69 Y.-Q. Zhang, X. Wang, H. Shi, F. Siddique, J. Xian, A. Song, B. Wang, Z. Wu and Z.-N. Cui, *J. Agric. Food Chem.*, 2024, **72**, 9611–9620.

70 W. H. Organization, *Marketing of Breast-Milk Substitutes: National Implementation of the International Code, Status Report 2020*, World Health Organization, 2020.

71 P. K. Deb, N. A. Al-Shar'i, K. N. Venugopala, M. Pillay and P. Borah, *J. Enzyme Inhib. Med. Chem.*, 2021, **36**, 869–884.

72 X. Duan, X. Xiang and J. Xie, *FEMS Microbiol. Lett.*, 2014, **360**, 87–99.

73 W. Li, A. Upadhyay, F. L. Fontes, E. J. North, Y. Wang, D. C. Crans, A. E. Grzegorzewicz, V. Jones, S. G. Franzblau, R. E. Lee, D. C. Crick and M. Jackson, *Antimicrob. Agents Chemother.*, 2014, **58**, 6413–6423.

74 A. D. H. Kingdon and L. J. Alderwick, *Comput. Struct. Biotechnol. J.*, 2021, **19**, 3708–3719.

75 Ö. Güzel-Akdemir, M. Trawally, M. Özbek-Babuç, B. Özbeçelik, G. Ermut and H. Özdemir, *Monatsh. Chem.*, 2020, **151**, 1443–1452.

76 Ö. Güzel, E. İlhan and A. Salman, *Monatsh. Chem.*, 2006, **137**, 795–801.

77 S. K. Pandey, A. Ahamd, O. P. Pandey and K. Nizamuddin, *J. Het. Chem.*, 2014, **51**, 1233–1239.

78 V. V. Vintonyak, K. Warburg, H. Kruse, S. Grimme, K. Hübel, D. Rauh and H. Waldmann, *Angew. Chem., Int. Ed.*, 2010, **49**, 5902–5905.

79 M. Trawally, K. Demir-Yazıcı, S. İ. Dingiş-Birgül, K. Kaya, A. Akdemir and Ö. Güzel-Akdemir, *Bioorg. Chem.*, 2022, **121**, 105688.

80 E. Krieghoff-Henning, J. Folkerts, A. Penzkofer and S. Weg-Remers, *Med. Monatsschr. Pharm.*, 2017, **40**, 48–54.

81 I. Peate, *Br. J. Health Care Manag.*, 2018, **12**, 350–355.

82 J. Ferlay, M. Colombet, I. Soerjomataram, D. M. Parkin, M. Piñeros, A. Znaor and F. Bray, *Int. J. Cancer*, 2021, **149**, 778–789.

83 M. M. Gottesman, *Annu. Rev. Med.*, 2002, **53**, 615–627.

84 M. Nikolaou, A. Pavlopoulou, A. G. Georgakilas and E. Kyrodimos, *Clin. Exp. Metastasis*, 2018, **35**, 309–318.

85 R. R. Love, H. Leventhal, D. V. Easterling and D. R. Nerenz, *Cancer*, 1989, **63**, 604–612.

86 P. Samadhiya, R. Sharma, S. K. Srivastava and S. D. Srivastava, *Arabian J. Chem.*, 2010, **7**, 657–665.

87 N. C. Desai, K. A. Jadeja, D. J. Jadeja, V. M. Khedkar and P. C. Jha, *Synth. Commun.*, 2021, **51**, 952–963.

88 K. Omar, A. Geronikaki, P. Zoumpoulakis, C. Camoutsis, M. Soković, A. Ćirić and J. Glamočlija, *Bioorg. Med. Chem.*, 2009, **18**, 426–432.

89 K. A. Szychowski, D. V. Kaminsky, M. L. Leja, A. P. Kryshchyshyn, R. B. Lesyk, J. Tobiasz, M. Wnuk, T. Pomianek and J. Gmiński, *Sci. Rep.*, 2019, **9**, 10609.

90 A. Türe, M. Ergül, M. Ergül, A. Altun and İ. Küçükgüzel, *Mol. Diversity*, 2020, **25**, 1025–1050.

91 Ö. Güzel-Akdemir and K. Demir-Yazıcı, *J. Res. Pharm.*, 2021, **25**(3), 305–317.

92 K. Demir-Yazıcı and Ö. Güzel-Akdemir, *J. Res. Pharm.*, 2022, **26**(4), 931–940.

93 M.-J. Hu, K. D. Cox, G. Schnabel and C.-X. Luo, *PLoS One*, 2011, **6**, e24990.

94 A. Uysal, P. Kinay-Teksür and D. Poyraz, *Plant Pathol. J.*, 2019, **101**, 773.

95 R. M. De Miccolis Angelini, G. Romanazzi, S. Pollastro, C. Rotolo, F. Faretra and L. Landi, *Genome Biol. Evol.*, 2019, **11**, 2850–2855.

96 R. M. De Miccolis Angelini, L. Landi, C. Raguseo, S. Pollastro, F. Faretra and G. Romanazzi, *Front. Microbiol.*, 2022, **13**, 854852.

97 T. T. Tran, H. Li, D. Q. Nguyen, K. Sivasithamparam, M. G. K. Jones and S. J. Wylie, *Australas. Plant Pathol.*, 2017, **46**, 339–349.

98 A. Foroumadi, S. Emami, A. Hassanzadeh, M. Rajaei, K. Sokhanvar, M. H. Moshafi and A. Shafiee, *Bioorg. Med. Chem. Lett.*, 2005, **15**, 4488–4492.

99 R. S. Upadhyaya, N. Sinha, S. Jain, N. Kishore, R. Chandra and S. K. Arora, *Bioorg. Med. Chem.*, 2004, **12**, 2225–2238.



100 H. Gao, X. Zhang, X.-J. Pu, X. Zheng, B. Liu, G.-X. Rao, C.-P. Wan and Z.-W. Mao, *Bioorg. Med. Chem. Lett.*, 2019, **29**, 806–810.

101 Q.-Y. Sun, W.-N. Zhang, J.-M. Xu, Y.-B. Cao, Q.-Y. Wu, D.-Z. Zhang, C.-M. Liu, S.-C. Yu and Y.-Y. Jiang, *Eur. J. Med. Chem.*, 2006, **42**, 1151–1157.

102 Y. Zhong, X. Li, A. Zhang, Y. Xu, P. Li and B. Wu, *Med. Chem. Res.*, 2018, **27**, 1366–1373.

103 Y. Zheng, D. Shi, D. Song, K. Chen, F. Wen, J. Zhang, W. Xue and Z. Wu, *Bioorg. Chem.*, 2024, **151**, 107647.

104 H.-R. Bjørsvik, L. Liguori and F. Minisci, *Org. Process Res. Dev.*, 2000, **4**, 534–543.

105 I. Favier, F. Giulieri, E. Duñach, D. Hébrault and J.-R. Desmurs, *Eur. J. Org. Chem.*, 2002, **2002**, 1984.

106 I. Favier and E. Duñach, *Tetrahedron*, 2003, **59**, 1823–1830.

107 A. Lesac, S. Narančić, M. Šepelj, D. W. Bruce and V. Šunjić, *Tetrahedron:Asymmetry*, 2003, **14**, 2731–2737.

108 C. Bolm, L. Zani, J. Rudolph and I. Schiffers, *Synthesis*, 2004, 2173–2180.

109 S. Barroso, G. Blay, L. Cardona, I. Fernández, B. García and J. R. Pedro, *J. Org. Chem.*, 2004, **69**, 6821–6829.

110 G. Blay, I. Fernández, B. Monje, M. C. Muñoz, J. R. Pedro and C. Vila, *Tetrahedron*, 2006, **62**, 9174–9182.

111 G. Blay, I. Fernández, B. Monje, M. Montesinos-Magraner and J. R. Pedro, *Tetrahedron*, 2010, **67**, 881–890.

112 S. P. M. Ventura, M. Gurbisz, M. Ghavre, F. M. M. Ferreira, F. Gonçalves, I. Beadham, B. Quilty, J. A. P. Coutinho and N. Gathergood, *ACS Sustainable Chem. Eng.*, 2013, **1**, 393–402.

113 H.-J. Jung, Y. S. Song, K. Kim, C.-J. Lim and E.-H. Park, *Arch. Pharmacal Res.*, 2010, **33**, 309–316.

114 F. Taran, P. Y. Renard, H. Bernard, C. Mioskowski, Y. Frobert, P. Pradelles and J. Grassi, *J. Am. Chem. Soc.*, 1998, **120**, 3332–3339.

115 A. Muheim and K. Lerch, *Appl. Microbiol. Biotechnol.*, 1999, **51**, 456–461.

116 X.-X. Pan, J.-J. Li, M.-G. Wang, W.-S. He, C.-S. Jia, X.-M. Zhang, B. Feng, D.-L. Li and Z. Zeng, *Biotechnol. Lett.*, 2013, **35**, 921–927.

117 R. Noyori, *Asymmetric Catalysis in Organic Synthesis*, Wiley-Interscience, 1994.

118 R. Liu, X. Bai, Z. Zhang and G. Zi, *Appl. Organomet. Chem.*, 2008, **22**, 671–675.

119 M. Dabiri, P. Salehi, G. Kozehgary, S. Heydari, A. Heydari and M. Esfandyari, *Tetrahedron:Asymmetry*, 2008, **19**, 1970–1972.

120 R. Faure, H. Loiseleur, R. Bartnik, S. Leśniak and A. Laurent, *Cryst. Struct. Commun.*, 1981, **10**, 515–519.

121 R. Bartnik, S. Lesniak and A. Laurent, *Tetrahedron Lett.*, 1981, **22**, 4811–4812.

122 S. Leśniak, M. Rachwalski, E. Sznajder and P. Kielbasiński, *Tetrahedron:Asymmetry*, 2009, **20**, 2311–2314.

123 M. Rachwalski, S. Jarzyński, M. Jasiński and S. Leśniak, *Tetrahedron:Asymmetry*, 2013, **24**, 689–693.

124 X. Liu, Z. Yi, J. Wang and G. Liu, *RSC Adv.*, 2015, **5**, 10641–10646.

125 H. Prydderch, A. Haiß, M. Spulak, B. Quilty, K. Kümmerer, A. Heise and N. Gathergood, *RSC Adv.*, 2017, **7**, 2115–2126.

126 A. Bergamo and G. Sava, *Chem. Soc. Rev.*, 2015, **44**, 8818–8835.

127 M. Gielen, *Tin Chemistry: Fundamentals, Frontiers, and Applications*, John Wiley & Sons, 2008.

128 T. S. B. Baul, D. Dutta, A. Duthie, R. Prasad, N. K. Rana, B. Koch and E. R. T. Tiekkari, *J. Inorg. Biochem.*, 2017, **173**, 79–92.

129 M. Nath, M. Vats and P. Roy, *Med. Chem. Res.*, 2014, **24**, 51–62.

130 S. Hadjikakou and N. Hadjiliadis, *Coord. Chem. Rev.*, 2008, **253**, 235–249.

131 C. E. Carraher and M. R. Roner, *J. Organomet. Chem.*, 2013, **751**, 67–82.

132 F. Arjmand, S. Parveen, S. Tabassum and C. Pettinari, *Inorg. Chim. Acta*, 2014, **423**, 26–37.

133 L. Niu, Y. Li and Q. Li, *Inorg. Chim. Acta*, 2014, **423**, 2–13.

134 M. Nath, *Appl. Organomet. Chem.*, 2008, **22**(10), 598–612.

135 M. Nath, M. Vats and P. Roy, *Eur. J. Med. Chem.*, 2012, **59**, 310–321.

136 M. Nath, M. Vats and P. Roy, *Inorg. Chim. Acta*, 2014, **423**, 70–82.

137 N. Mridula and M. Nath, *J. Photochem. Photobiol. B*, 2016, **162**, 348–360.

138 M. Nath, P. Roy, R. Mishra and M. Thakur, *Appl. Organomet. Chem.*, 2019, **33**, e4663.

139 P. Muthuraja, R. Usman, R. Sajeev and P. Gopinath, *Org. Lett.*, 2021, **23**, 6014–6018.

140 M. Sharon, A. Durve, A. Pandey and M. Pathak, *Mandelic Acid: Aha*, Partridge Publishing, 2018.

141 K. Kacprzak, N. Maier and W. Lindner, *J. Sep. Sci.*, 2010, **33**, 2590–2598.

142 M.-Y. Nie, L.-M. Zhou, Q.-H. Wang and D.-Q. Zhu, *Anal. Sci.*, 2001, **17**, 1183–1187.

143 W. A. König, *Gas Chromatographic Enantiomer Separation with Modified Cyclodextrins*, 1992.

144 Z. Juvancz, R. Bodáné-Kendrovics, L. Szente and D. Maklári, *Period. Polytech., Chem. Eng.*, 2021, **65**, 580–594.

145 H. Schmarr, A. Mosandl and A. Kaunzinger, *J. Microcolumn Sep.*, 1991, **3**, 395–402.

146 C. Bicchi, A. D'Amato, V. Manzin, A. Galli and M. Galli, *J. Chromatogr. A*, 1994, **666**, 137–146.

147 F. Kobor, K. Angermund and G. Schomburg, *J. High Resolut. Chromatogr.*, 1993, **16**, 299–311.

148 F. Kobor and G. Schomburg, *J. High Resolut. Chromatogr.*, 1993, **16**, 693–699.

149 L. Repassy, Z. Juvancz, R. Bodáné-Kendrovics, Z. Kaleta, C. Hunyadi and G. Riszter, *Int. J. Mol. Sci.*, 2023, **24**, 15051.

150 M. M. E. Shakdofa, M. H. Shtaiwi, N. Morsy and T. M. A. Abdel-Rassel, *Main Group Chem.*, 2014, **13**, 187–218.

151 M. K. Hossain, M. O. Plutenko, J. A. Schachner, M. Haukka, N. C. Mösch-Zanetti, I. O. Fritsky and E. Nordlander, *J. Indian Chem. Soc.*, 2021, **98**, 100006.

152 A. D. M. Mohamad, M. J. A. Abualreish and A. M. Abu-Dief, *J. Mol. Liq.*, 2019, **290**, 111162.



153 A. M. Abu-Dieff, R. M. El-Khatib, S. M. E. Sayed, S. Alzahrani, F. Alkhatab, G. El-Sarrag and M. Ismael, *J. Mol. Struct.*, 2021, **1244**, 131017.

154 M. Jabeen, *J. Turk. Chem. Soc., Sect. A*, 2022, **9**, 663–698.

155 M. Bagherzadeh, M. Zare, V. Amani, A. Ellern and L. K. Woo, *Polyhedron*, 2013, **53**, 223–229.

156 O. Pouralimardan, A.-C. Chamayou, C. Janiak and H. Hosseini-Monfared, *Inorg. Chim. Acta*, 2006, **360**, 1599–1608.

157 S. Balgotra, P. K. Verma, R. A. Vishwakarma and S. D. Sawant, *Catal. Rev.*, 2019, **62**, 406–479.

158 W. Xiao, Z.-L. Lu, C.-Y. Su, K.-B. Yu, L.-R. Deng, H.-Q. Liu and B.-S. Kang, *J. Mol. Struct.*, 2000, **553**, 91–99.

159 J. Patole, U. Sandbhor, S. Padhye, D. N. Deobagkar, C. E. Anson and A. Powell, *Bioorg. Med. Chem. Lett.*, 2003, **13**, 51–55.

160 M. M. Najafpour, B. Pashaei and Z. Zand, *Dalton Trans.*, 2013, **42**, 4772.

161 N. Schuth, Z. Liang, M. Schönborn, A. Kussicke, R. Assunção, I. Zaharieva, Y. Zilliges and H. Dau, *Biochemistry*, 2017, **56**, 6240–6256.

162 A. Das, M. Chakraborty, S. Maity and A. Ghosh, *Dalton Trans.*, 2019, **48**, 9342–9356.

163 S. K. Fathalla, H. A. El-Ghamry and M. Gaber, *Inorg. Chem. Commun.*, 2021, **129**, 108616.

164 A. Panja, M. Shyamal, A. Saha and T. K. Mandal, *Dalton Trans.*, 2014, **43**, 5443.

165 A. Panja, *Dalton Trans.*, 2014, **43**, 7760.

166 H. A. El-Ghamry, M. Gaber, F. M. Alkhatab, H. F. A. Shareef, K. M. Takroni and S. K. Fathalla, *RSC Adv.*, 2024, **14**, 30673–30686.

167 P. S. Kumar, A. Banerjee and S. Baskaran, *Angew. Chem.*, 2009, **122**, 816–819.

168 G. I. Matsumoto, M. Shioya and H. Nagashima, *Phytochemistry*, 1984, **23**, 1421–1423.

169 M. Bousquet, R. Willemot, P. Monsan and E. Boures, *Biotechnol. Bioeng.*, 1999, **62**, 225–234.

